Geochemistry Geophysics Geosystems G3
AN ELECTRONIC JOURNAL OF THE EARTH SCIENCES
Published by AGU and the Geochemical Society

Article
Volume 8, Number 3
15 March 2007
Q03P21, doi:10.1029/2006GC001425
ISSN: 1525-2027

New spatial Mg/Ca-temperature calibrations for three Arctic, benthic foraminifera and reconstruction of north Iceland shelf temperature for the past 4000 years

G. B. Kristjánsdóttir
Institute of Arctic and Alpine Research (INSTAAR) and Department of Geological Sciences, University of Colorado, Boulder, Colorado 80309-0450, USA

Now at The Godwin Laboratory for Palaeoclimate Research, Department of Earth Sciences, University of Cambridge, Downing Street, Cambridge CB2 3EQ, UK (gkri05@esc.cam.ac.uk)

D. W. Lea
Department of Earth Science and Marine Science Institute, University of California, Santa Barbara, CA 93106-9630, USA

A. E. Jennings
Institute of Arctic and Alpine Research (INSTAAR) and Department of Geological Sciences, University of Colorado, Boulder, Colorado 80309-0450, USA

D. K. Pak and C. Belanger
Department of Earth Science and Marine Science Institute, University of California, Santa Barbara, California 93106-9630, USA

[1] We have developed cold-end Mg/Ca-temperature calibrations for three common Arctic benthic foraminifera, *Islandiella norcrossi/helenae*, *Melonis barleeanus*, and *Cassidulina neoteretis*, and compare the three calibrations in a late Holocene downcore record (0–4000 cal yr B.P.). The calibration and downcore trends for the three Arctic species extend the observation that Mg incorporation into benthic foraminifera is species specific. For the calibration we use a set of CTD casts, bottom water $\delta^{18}O_{seawater}$ measurements, and surface grab-samples collected from the Iceland margin (cruise B997) and the Greenland margin (cruise BS1191). Water depth of sites used ranges from 165 to 656 m, while spatial bottom temperature ranges from 0 to 7°C. Mg/Ca values ranged from 1.02 to 1.47 for *I. norcrossi*/*helenae*, 0.64 to 2.21 for *M. barleeanus*, and 0.93 to 1.38 mmol/mol for *C. neoteretis*. We calibrated Mg/Ca content against isotopic calcification temperature (calculated using $T = 16.9 - 4.0*(\delta^{18}O_{calcite\ corrected\ for\ vital\ effect} - \delta^{18}O_{seawater})$). Exponential calibrations for the three species are as follows: *I. norcrossi*/*helenae* Mg/Ca = 1.051 ± 0.03 * exp(0.060 ± 0.011 * T), *M. barleeanus* Mg/Ca = 0.658 ± 0.07 * exp(0.137 ± 0.020 * T), and *C. neoteretis* Mg/Ca = 0.864 ± 0.07 * exp(0.082 ± 0.020 * T). On the basis of Mg/Ca in these benthic species the downcore record from core MD99-2269 is reconstructed. Bottom temperature values are interpreted to reflect variable inflow of Atlantic and Arctic water to the north Iceland shelf during the last 4000 cal yr B.P. All three reconstructions show a decline by 0.1°C per century from circa 1500-0 cal yr B.P., which coincides with an increase in Arctic benthic foraminifera abundances and a rise in sea ice proxies in the same core. Intriguingly, *C. neoteretis* diverges periodically to higher average temperature (Atlantic water conditions) than shown by *M. barleeanus* or *I. norcrossi*/*helenae* (which both show Arctic water temperature) circa 1500–4000 cal yr B.P.

Components: 11,100 words, 10 figures, 4 tables.

Keywords: Mg/Ca; benthic foraminifera; temperature calibrations; Arctic; shelf environment; Iceland shelf.

Index Terms: 1065 Geochemistry: Major and trace element geochemistry; 4924 Paleoceanography: Geochemical tracers; 9325 Geographic Location: Atlantic Ocean.

Received 20 July 2006; **Revised** 14 November 2006; **Accepted** 29 November 2006; **Published** 15 March 2007.

Kristjánsdóttir, G. B., D. W. Lea, A. E. Jennings, D. K. Pak, and C. Belanger (2007), New spatial Mg/Ca-temperature calibrations for three Arctic, benthic foraminifera and reconstruction of north Iceland shelf temperature for the past 4000 years, *Geochem. Geophys. Geosyst.*, *8*, Q03P21, doi:10.1029/2006GC001425.

Theme: Development of the Foraminiferal Mg/Ca Proxy for Paleoceanography
Guest Editor: P. Martin

1. Introduction

[2] Arctic continental-shelf sediments have been shown to be sensitive and potentially very high-resolution recorders of paleoclimatic and paleoceanographic changes. However, one of the main problems in Arctic paleoceanography is the lack of good, quantitative proxies for both temperature and salinity, particularly for benthic conditions. Advances in Mg/Ca studies of foraminifera (and ostracods) may provide us with the ideal quantitative proxy that can be used to reconstruct both sea surface and bottom water conditions. Calibrations of Mg/Ca ratio against temperature are reasonably well-constrained for planktonic foraminifera at temperatures above 10°C but are less well developed for benthic foraminifera and cooler temperatures, thus currently limiting the method's applicability to high-latitude and deep water studies. Despite the smaller changes predicted by the theoretical exponential relationship between temperature and Mg incorporation, cold end Mg/Ca benthic records appear to record significant paleotemperature variations [*Martin et al.*, 2002; *Marchitto and deMenocal*, 2003; *Skinner et al.*, 2003] although the carbonate ion effect must be considered for deep water reconstructions [*Elderfield et al.*, 2006]. Previous studies have shown that the Mg/Ca-temperature response and relationship in benthic foraminifera is species specific [*Izuka*, 1988; *Rathburn and De Deckker*, 1997; *Rosenthal et al.*, 1997; *Lear et al.*, 2000, 2002; *Toyofuku et al.*, 2000; *Billups and Schrag*, 2002; *Martin et al.*, 2002; *Hintz et al.*, 2006b; *Elderfield et al.*, 2006]. Therefore single species calibrations will offer the most accurate temperature reconstructions. Core top and culture calibrations for different benthic species are emerging (Table 1) but many of the calibrations have few data points and cover only a limited temperature range making it difficult to discern the true relationship, be it exponential or linear, between Mg/Ca and temperature and perhaps also the carbonate ion. Here we calibrate the Mg/Ca-temperature relationship of three benthic foraminifera species living on Arctic continental shelves and focus on strengthening the calibration at low temperatures by using a robust, shallow-water (presumably unaffected by carbonate ion effect), data set from the west and north Iceland shelf and the east Greenland shelf. The Iceland and Greenland margins, near the northern limit of Atlantic water, have a spatial temperature range of 0 to 7°C and are thus an ideal location to conduct cool water calibrations for Mg/Ca studies. The new benthic calibrations were then applied to Mg/Ca measurements of all three species in a 4000 cal yr B.P. downcore record from the north Iceland shelf.

2. Hydrographic Setting: Modern Oceanographic Conditions

[3] Two main surface currents converge on the Iceland shelf (water depth approximately 100–680 m). The East Icelandic Current (EIC) carrying Arctic and/or Polar water masses from the north and the Irminger Current (IC) carrying warmer Atlantic water from the south. As the Irminger Current rounds the tip of Iceland and flows into the north Iceland shelf it is termed the North Iceland Irminger Current (NIIC) (Figure 1). Atlantic water of the Irminger Current occupies the whole water column on the southwest and west Iceland shelf (Figure 2a; Jökuldjúp and Djúpáll) resulting in relatively stable seasonal and annual conditions with bottom water

Table 1. Available Mg/Ca-Temperature Relationships and Calibrations for Benthic Foraminifera[a]

Species	T Range, °C	Mg/Ca, mmol/mol	Mg/Ca = B × exp (A × T): B	A	n	R^2	Error of Estimate	Sample Type	Instrument	Cleaning Method[b]	Water Depth, m	Reference
Islandiella norcrossi/helenae	0.21–5.25	1.02–1.47	1.051 (±0.03)	0.060 (±0.011)	15	0.93	±0.63	surface samples	ICP-MS	Full	162–501	(1) this study
Cassidulina neoteretis	0.96–5.47	0.93–1.38	0.864 (±0.07)	0.082 (±0.020)	10	0.9	±0.62	surface samples	ICP-MS	Full	211–483	(2) this study
Melonis barleeanus	0.19–6.99	0.64–2.21	0.658 (±0.07)	0.137 (±0.020)	31	0.81	±1.10	surface samples	ICP-MS	Full	211–637	(3) this study
Melonis barleeanus, composite calibration	0.19–18.38	0.64–6.01	0.757 (±0.09)	0.119 (±0.014)	43	0.9	±1.84	surface samples	ICP-MS	Full	211–2546	(4) this study and data from *Lear et al.* [2002]
M. barleeanus and *M. pompilioides*	0.8–18.4	-	0.982	0.101	42	0.84	-	core tops	ICP-MS/AES, FAAS?	-	-	(5) *Lear et al.* [2002]
Cibicidoides spp	0.8–18.4	~0.92–7.18	0.867 (±0.049)	0.109 (±0.007)	101	0.94	±1.7	core tops	ICP-MS/AES, FAAS	Mix	-	(6) *Lear et al.* [2002]
Cibicidoides spp	>5	~1.68–7.18	1.009 (±0.187)	0.097 (±0.132)	-	0.84	±1.3	core tops	ICP-MS/AES, FAAS	Mix	-	*Lear et al.* [2002]
Cib. pachyderma and *Cib. wuellerstorfi*	0.4–18 (tbl) −1.1–18(text)	-	1.22(±0.08)	0.109(±0.007)	-	0.95	±1.4	core tops	Mix	Mix	301–4920	*Martin et al.* [2002]
Cib. pachyderma and *Cib. wuellerstorfi*	-	-	0.85	0.11	-	-	-	modified C. spp. equat.	-	-	-	(7) *Martin et al.* [2002]
Cibicidoides mundulus	-	-	0.9	0.11	-	-	±1	modified C. spp. equat.	-	-	-	*Lear et al.* [2003]
Cibicidoides floridanus	4.5–18.38	2.17–10.24	1.36	0.1	20	-	-	core tops	FAAS	Leach	301–1243	(8) *Rosenthal et al.* [1997] as cited by *Lear et al.* [2002]
Globobulimina affinis	−1.6–3.28	2.3–4.5	2.91 (±0.05)	0.08 (±0.007)	22	0.93	-	downcore samples	ICP-AES	Soft	3146	(9) *Skinner et al.* [2003]
Oridorsalis umbonatus	0.8–9.9	-	1.008	0.114	23	0.4	-	core tops	ICP-MS/AES	Full?	-	*Lear et al.* [2002]
Oridorsalis umbonatus	-	-	1.06	0.1	-	-		modified C. spp. equat.	ICP-AES	Soft	-	*Lear et al.* [2000]
Planulina ariminensis	3.0–14.5	-	0.911	0.062	10	0.69	-	core tops	ICP-MS	Full?	-	(10) *Lear et al.* [2002]
Planulina spp	2.3–12.0	-	0.788	0.119	7	0.96	-	core tops	ICP-MS	Full?	-	*Lear et al.* [2002]
Uvigerina spp	1.8–18.4	-	0.924	0.061	58	0.69	-	core tops	ICP-MS	Full?	-	(11) *Lear et al.* [2002]
Marginopora kudakajimaensis	21–29	258.2–361.8	143.18	0.0317	18	0.74	-	collected alive	ICP-AES	Soft	2	*Raja et al.* [2005]

Species	T Range, °C	Mg/Ca, mmol/mol	Temperature Relationship: Mg/Ca =	n	R^2	Error of Estimate	Sample Type	Instrument	Cleaning Method[b]	Water Depth, m	Reference
Archaias angulatus	22–29	~110–130	= 0.21T+6.4	4	0.66	-	collected alive	ICP-MS	Rinsed in NaOCl	-	*Toler et al.* [2001]
Amphistegina gibbosa	22–29	20–40	no significant relationship	6	-	-	collected alive	ICP-MS	Rinsed in NaOCl	-	*Toler et al.* [2001]
B. aculeata	4.4–8.9	-	$D_{Mg} = 0.290e^{0.104T}$	11	-	-	culture and core tops	HR-ICP-MS	Full/soft	210–1020	*Hintz et al.* [2006b]
Cassidulina subglobosa	~2–20		not given, just comment it is similar to temperature				core tops	Microprobe	Polishing	260–4332	*Izuka* [1988]
Cassidulina oriangulata	~9–30		not given, just comment it is similar to temperature				core tops	Microprobe	Polishing	102–399	*Izuka* [1988]
Cibicidoides pachyderma	4–18	1–5.5	= 0.25T + 0.35	12	0.88	-	core tops	ICP-MS	Full	-	(12) *Marchitto and DeMenocal* [2003]
2 Cib.flor/1 Cib.wuell.	1.6–5.34	1.37–2.5	= 0.32T + 0.76	3	-	-	core tops	ICP-AES, FAAS	Mix	1043–2500	*Billups and Schrag* [2002]
Cibicidoides pachyderma (floridanus)	4.5–18.38	2.17–10.24	$= 1.36 * 10^{0.044T}$	20	0.92	±0.85	core tops	FAAS	Not full	301–1243	*Rosenthal et al.* [1997]
Cibicides wuellerstorfi	2.25–5.87	~2–3.5	= 0.342T + 1.39	5	0.78	-	core tops	GFAAS	Sonication	792–2038	*Rathburn and De Deckker* [1997]
Cibicides wuellerstorfi, Cibicides refulgens	−1.92–5.87	~1.25–3.5	= 0.277T + 1.73	10	0.88	-	core tops	GFAAS	Sonication	200–2038	*Rathburn and De Deckker* [1997]

Table 1. (continued)

Species	T Range, °C	Mg/Ca, mmol/mol	Temperature Relationship: Mg/Ca =	n	R^2	Error of Estimate	Sample Type	Instrument	Cleaning Method[b]	Water Depth, m	Reference
H. elegans in oversat. waters with respect to arag.	4.2–18.4	1.01–1.95	= (0.034 ± 0.002)T + 0.96 ± 0.03)	49	0.82	±1.1	core tops	ICP-MS	Full	301–1585	*Rosenthal et al.* [2006]
Planoglabratella opercularis	10.4–23.1	97.3–118.4	= 1.6T + 81.5	7	0.98	-	culture	Microprobe	Polishing	Very shallow	*Toyofuku and Kitazato* [2005]
Planoglabratella opercularis	9.8–23.1	114–149	= 2.22T + 89.69	4	0.98	-	culture	ICP-MS/AES	Not full	Very shallow	*Toyofuku et al.* [2000]
Quinqueloculina yabei	9.7–24.5	93–136	= 2.90T + 65.98	4	1.00	-	culture	ICP-MS/AES	Not full	Very shallow	*Toyofuku et al.* [2000]
Trifarina angulosa	−1.92–0.19	0.81–3.74	possible relationship	13	-	-	core tops	GFAAS	Sonication	200–880	*Rathburn and De Deckker* [1997]
Uvigerina spp.	−2–9	1–5	perhaps some in *U. peregrina*	11	-	-	core tops	GFAAS	Sonication	562–2038	*Rathburn and De Deckker* [1997]

[a] For this study, errors on A and B are 95% CI. Numbers in parenthesis (1–12) in the last column refer to Figure 8b. A dash ("-") indicates that either data were not given in paper or there was some ambiguity as to what exact data points were used to construct the calibration.

[b] Full cleaning, trace metal cleaning including a reductive step (see text); Soft cleaning, trace metal cleaning without a reductive step; Mix, more than one cleaning method used to clean the samples.

temperatures ranging from 7 to 10°C [*Malmberg and Kristmannsson*, 1992]. On the north Iceland shelf Atlantic water of the NIIC converges with Arctic and/or Polar water of the EIC resulting in a stratified water column (Figure 2a; Reykjafjardaráll-Húnaflóadjúp and Eyjafjarðaráll, Figure 3). Bottom water temperature may vary from ≤0 to around 5°C, depending on the dominant water mass at the seafloor. The inner shelf tends to be overlain by Atlantic water of the NIIC whereas the outer shelf is more often bathed in upper Arctic Intermediate water (formed by convection in the Iceland and Greenland Seas [*Swift and Aagaard*, 1981; *Malmberg and Kristmannsson*, 1992]). Nearshore the Atlantic water of the NIIC is overlain by seasonally warmed, low salinity coastal water, whereas offshore it is submerged beneath the EIC carrying either or both Arctic and Polar water to the north Iceland shelf [*Swift and Aagaard*, 1981; *Hopkins*, 1991; *Malmberg and Kristmannsson*, 1992; *Malmberg and Jónsson*, 1997]. This stratification and change from inner to outer shelf is well displayed in the 1997 hydrographic data in Figure 2a and benthic foraminiferal fauna variations [*Jennings et al.*, 2004] in Figure 4.

[4] The stratification of the North Iceland shelf varies from season to season and year to year. A time series of recent hydrographic changes at the Siglunes (Figure 1) hydrographic station (http://www.hafro.is/Sjora/) illustrates clearly the annual variability and regime changes that may occur on the North Iceland shelf. Atlantic water of the NIIC dominated the North Iceland shelf region prior to 1965 but was replaced by varying Polar, Arctic or Atlantic conditions after 1965 (Figure 3) [*Malmberg and Jónsson*, 1997]. Inflow of Atlantic water of the NIIC supplies both heat and nutrients to the north Iceland shelf [*Ólafsson*, 1999] and therefore diminished NIIC inflow in the cold years after 1965 resulted in diminished primary productivity [*Thordardóttir*, 1977; *Ólafsson*, 1985]. The year of the B997 cruise (1997) was a relatively average year with regard to both temperature and salinity (Figure 3). However, spring and winter of 1995, two years prior to the B997 cruise, exhibited exceptionally low temperatures (0°C, <34.6–34.8 psu) on the north shelf [*Malmberg and Jónsson*, 1997; *Jónsson and Briem*, 2003].

[5] Site MD99-2269 is located in the path of Atlantic water inflow to the North Iceland shelf [*Labeyrie et al.*, 2003] and thus is ideal to monitor changes in inflow of NIIC to the north Iceland shelf. Our hypothesis is that an increase in bottom water temperature over MD99-2269 is the result

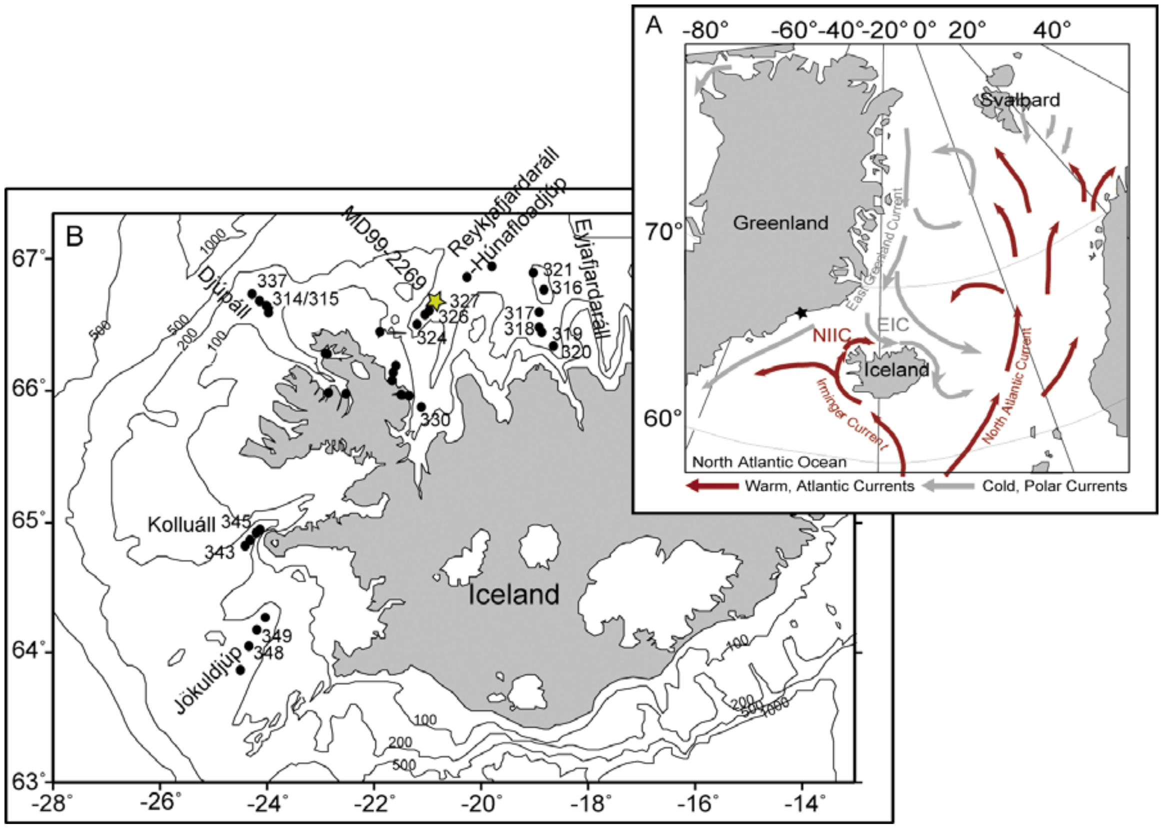

Figure 1. Location of sample sites. (a) Simplified figure of surface currents in the North Atlantic, warm currents in red, cold currents in light gray. A star indicates location of Greenland site K15 (off Nansen fjord). (b) Bathymetry and site locations on the Iceland shelf. Circles indicate B997 sites, and a star denotes site MD99-2269. Unmarked circles are B997 sites, which were not used in this study. Location of hydrographic station Siglunes-3 (S-3, Figure 3) is close to site 317 on the north Iceland shelf.

of greater NIIC inflow to the north shelf. A stronger inflow of warm Atlantic water induces a warmer climate for northern Iceland, influencing vegetation and local glaciers in the area.

[6] The Greenland shelf, off Nansen fjord (water depth 445 m), is overlain by the East Greenland Current (EGC) (Figure 1a). EGC is composed of Atlantic Intermediate water (AIW) overlain by fresh Polar water (PW) [*Aagaard and Coachman*, 1968a, 1968b; *Johannessen*, 1986]. AIW at this site originates from the southward turning branch of the West Spitzbergen Current and southward flow of Atlantic layer from the Arctic Ocean [*Aagaard and Coachman*, 1968a, 1968b]. Bottom water temperatures vary between 0 and 4°C.

3. Materials and Methods

3.1. Modern Calibration Samples

[7] Modern surface-sediment samples from the Iceland shelf were collected in July 1997 during cruise B997 (R/V *Bjarni Sæmundsson* RE 30). Samples were collected from 40 sites along the southwest, northwest and north Iceland shelf and fjords (Figure 1b). Water depth at these sites ranged 40–660 m [*Helgadóttir*, 1997]. From the 40 sites we excluded sites with low abundances (or total absence) of the species under study, these included all fjord sites and some shelf sites. The remaining 17 shelf sites (water depth 165–656 m) were used for this study (Table 2, Figure 1b). Surface-sediment samples were collected at the water/sediment interface with a Shipek sediment-sampler. The water/sediment interface was easily distinguishable as a brown or greenish soupy sediment layer containing living macrofauna. Samples with an undisturbed surface were sub-sampled by scraping of the top 1 cm. Samples were stained with Rose Bengal immediately upon collection and later wet sieved to >63 μm and then dry sieved to >106 μm. Surface-sediment samples from the Greenland margin were collected with a Shipek sediment-sampler during cruises BS1191 and HU93030 in 1991 and 1993 respectively. Only one sample,

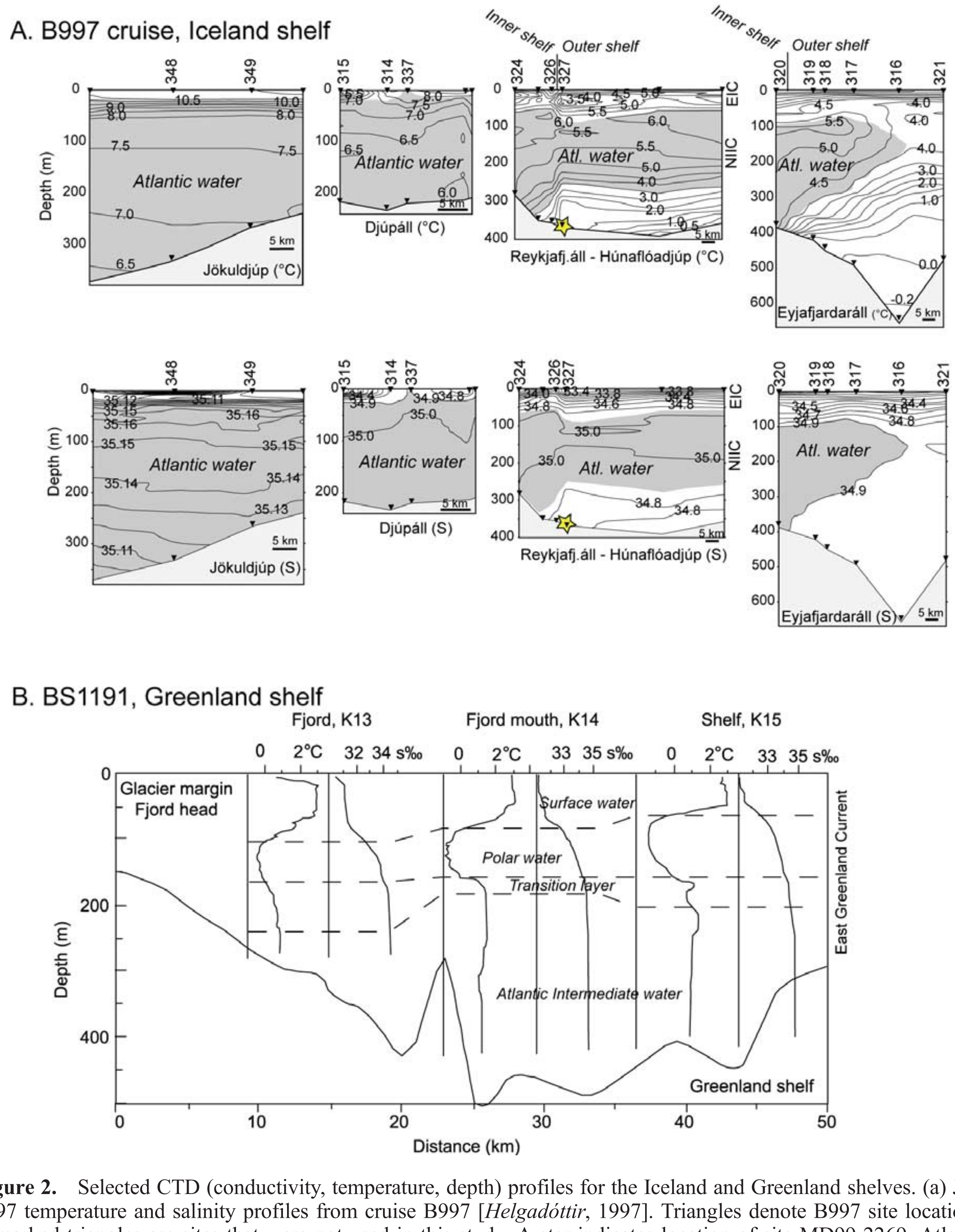

Figure 2. Selected CTD (conductivity, temperature, depth) profiles for the Iceland and Greenland shelves. (a) July 1997 temperature and salinity profiles from cruise B997 [*Helgadóttir*, 1997]. Triangles denote B997 site locations; unmarked triangles are sites that were not used in this study. A star indicates location of site MD99-2269. Atlantic water (>34.9 psu and >3.5°C) of the IC and NIIC is outlined in gray. Note that the Atlantic water occupies an intermediate position in the water column on the north shelf and in July 1997 site MD99-2269 is not bathed in Atlantic water. The B997 CTD data correlate well with hydrographic data collected seasonally by the Marine Institute in Iceland http://www.hafro.is/Sjora/). (b) October 1991 temperature and salinity profiles from cruise BS1191 [*Andrews et al.*, 1991]. Graph is modified from *Jennings and Weiner* [1996].

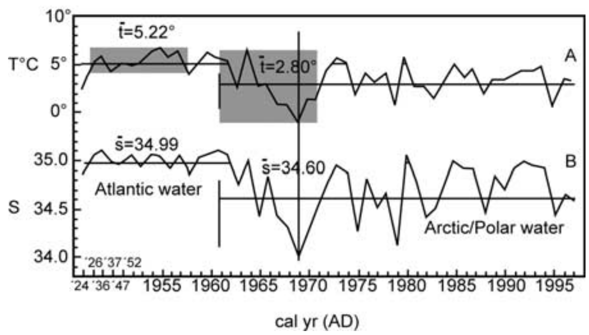

Figure 3. May/June time series of (a) temperature and (b) salinity variations at 50 m depth in north Icelandic waters (Siglunes hydrographic station S-3) [*Malmberg and Jónsson*, 1997], with additional data from http://www.hafro.is/Sjora/. Site S-3 is located by B997 site 317 in Figure 1b. Notice the change from dominantly Atlantic waters prior to 1962–1964 to dominantly Polar waters after 1964 and a slow rise back toward Atlantic conditions with 1995 as a cold year. Gray blocks represent the potential variability one might encounter in a sediment sample spanning 8 years (see discussion in text).

BS11-91-K15, from the Greenland shelf had enough calcareous foraminifera for Mg/Ca analysis. Water depth at the Greenland site was 445 m (Table 2).

[8] Three species of benthic foraminifera (*Islandiella norcrossi/helenae*, *Melonis barleeanus*, and *Cassidulina neoteretis*) were picked from the >106 μm fractions. Both pristine stained and pristine unstained tests were picked, as there were a limited number of stained tests in the samples. Due to the small size and limited number of foraminifera in the samples we were not able to limit the study to a single, narrow, size fraction (see discussion later). Great care was taken to pick only tests that showed no signs of dissolution, fragmentation, or dirty chambers. Before analysis each Mg/Ca sample (9–113 tests) went through the full (also termed hard) trace metal cleaning as designed by *Boyle and Keigwin* [1985/1986] and subsequently modified [*Boyle and Rosenthal*, 1996; *Martin and Lea*, 2002]. This cleaning procedure requires a sample size of at least 0.175 mg for optimal recovery. Briefly, shells were cracked open between glass plates to expose inner chambers to the cleaning reagents and loaded into 0.6 ml microcentrifuge tubes. Samples were subjected to the following: (1) Seven aggregate rinses (three ultra pure water (n-pure) rinses, two methanol rinses and two additional ultra pure water rinses) to remove clays and adsorbing material. All rinses, except the last ultra pure water rinse included 30 sec of ultrasonication.

Table 2. Logistic Information for B997 Sites, Site MD99-2269, and Site K15

Cruise	Site	Site Location	Site Descr.	Latitude, N	Longitude, W	Grab Depth, m	BWT,[a] °C	BWS,[b] psu	$\delta^{18}O_{seawater\ VSMOW}$, ‰
				Iceland Shelf					
B997	314	Djúpáll	shelf	66°41.000′	24°10.800′	233	6.0	35.05	0.28
B997	315	Djúpáll	shelf	66°44.000′	24°19.900′	217	6.0	35.05	0.23
B997	316	Eyjafjardaráll	shelf	66°45.040′	18°47.530′	656	−0.2	34.88	0.15
B997	317	Eyjafjardaráll	shelf	66°35.330′	18°51.940′	495	−0.1	34.88	0.23
B997	318	Eyjafjardaráll	shelf	66°29.240′	18°53.140′	452	0.1	34.87	0.19
B997	319	Eyjafjardaráll	shelf	66°26.950′	18°50.550′	422	0.2	34.87	0.2
B997	320	Eyjafjardaráll	shelf	66°20.000′	18°39.500′	385	4.7	34.95	0.16
B997	321	Eyjafjardaráll	shelf	66°53.395′	18°58.675′	487	0.2	34.87	0.23
B997	324	Reykjafjardaráll	shelf	66°31.450′	21°09.110′	281	5.5	35.00	0.28
B997	325	Reykjafjardaráll	shelf	66°34.403′	20°59.837′	350	3.2	34.82	0.2
B997	327	Reykjafjardaráll	shelf	66°38.267′	20°51.956′	368	1.6	34.78	0.16
B997	330	Húnaflóaáll	shelf	65°52.016′	21°04.913′	165	5.3	34.86	0.15
B997	337	Djúpáll	shelf	66°40.056′	24°07.544′	220	6.2	35.07	0.28
B997	343	Kolluáll	shelf	64°46.604′	24°29.306′	273	6.4	35.09	0.3
B997	345	Kolluáll	shelf	64°52.716′	24°15.481′	322	no CTD[c]	no CTD[c]	0.29
B997	346	Kolluáll	shelf	64°55.615′	24°07.707′	320	7.1	35.11	0.23
B997	348	Jökuldjúp	shelf	64°04.563′	24°19.371′	327	6.8	35.12	0.31
B997	349	Jökuldjúp	shelf	64°12.538′	24°10.044′	266	7.0	35.13	0.28
MD99	2269	Reykjafjardaráll	shelf	66°37.53′	20°51.16′	365	NA	NA	NA
				Greenland Shelf					
BS1191	K15	Off Nansen fjord	shelf	68°06.02′	29°27.16′	445	1.0	34.75	NA

[a] BWT, bottom water temperature from B997-CTD.
[b] BWS, bottom water salinity from B997-CTD.
[c] Used T and S data from the nearby site 346.

(2) Reduction with 100 μl of a hydrazine solution (750 μl anhydrous hydrazine in 10 ml of ammonium citrate and 10 ml of NH_4OH) in a hot water bath for 30 min, with 2–3 sec ultrasonication every 2 min. (3) Oxidation with 250 μl of buffered peroxide solution (300 μl 30% H_2O_2 in 30 ml 0.1 N NaOH) in a hot water bath for 10 min with two 2–3 sec ultrasonication periods. (4) A final leach with 250 μl, 100 μl or no dilute nitric acid (0.001 N $HN0_3$), depending on the size of the remaining sample, followed by a final ultra pure water rinse. Cleaned samples were run on an ICP-MS at the University of California, Santa Barbara. Results are reported in mmol/mol or μmol/mol. Analytical error for Mg/Ca is estimated at ±1% (RSD) or better, which is equivalent to approximately 0.02 mmol/mol (2 sigma). Elemental ratios of Fe/Ca and Al/Ca (detrital phases) and Mn/Ca (secondary coatings) were analyzed at the same time as Mg/Ca. The first two (measured in medium resolution) were determined by direct reference to the two isotopes used for quantification of calcium, ^{43}Ca and ^{48}Ca [*Lea et al.*, 2005]. Analytical error for Mn/Ca based on matched consistency standards is estimated at 1.4%. Errors for Al/Ca and Fe/Ca determination are estimated at <5%. In addition Sr, Na, Cd, Ba, La, Ce, Nd, Eu, Lu, and U were measured in the samples, but are not reported here.

[9] Separate samples for δ^{18}O analysis were sent to the Leibniz-Laboratory for Radiometric Dating and stable isotope research at Christian-Albrechts-University Kiel, Germany. The numbers of tests varied from 7 to 40 depending on their size, but in general between 20 and 30 specimens were run for each sample (Table 3). Isotopic analysis was performed using a Finnigan MAT 251 mass spectrometer with an on-line coupled Kiel Carbon device. The results are defined in the conventional δ-notation in ‰ ($\delta^{18}O_{calcite}$) relative to VPDB. Analytical error of the measurements is better than 0.06 ‰.

3.2. Hydrographic Data

[10] Modern hydrographic data for the Iceland shelf, at seasonal resolution, are available at http://www.hafro.is/Sjora/. CTD casts were also taken at each station during cruises BS11-91 [*Andrews et al.*, 1991] and B997 [*Helgadóttir*, 1997]. Bottom water samples for $\delta^{18}O_{seawater}$ analysis were taken at most stations during the B997 cruise. $\delta^{18}O_{seawater}$ measurements were done at the Science Institute, University of Iceland where oxygen was extracted from the water samples after the method of *Epstein and Mayeda* [1953]. Stable isotope analyses for oxygen were performed on a Finnegan MAT 251 mass-spectrometer. The results are defined in the conventional δ-notation in ‰ relative to VSMOW. The analytical error of the measurements is <0.05 ‰. We use the −0.27 ‰ conversion of *Hut* [1987] to convert $\delta^{18}O_{seawaterVSMOW}$ to $\delta^{18}O_{seawaterVPDB}$. The carbonate saturation state of bottom waters was not measured for this study, but due to the shallow environment we assume they are oversaturated. *Elderfield et al.* [2006] found the modern conditions in the Norwegian Sea to be highly saturated.

3.3. Downcore Samples

[11] Core MD99-2269 was collected in 1999 during the IMAGES V cruise aboard R/V *Marion Dufresne* [*Labeyrie et al.*, 2003]. Site MD99-2269 is located in 365 m water depth (Table 2) in Reykjafjardaráll, north Iceland shelf (66°37.53′N, 20°51.16′W). The core is a ~25 m long Calypso piston-core bottoming out in the Vedde tephra circa 12,000 cal yr B.P. with a modern coretop. The age model (PSV-RC06) for the core is based on 44 radiocarbon dates and paleomagnetic synchronization of cores MD99-2269 and MD99-2322 (67°08.18′N, 30°49.67′W) [*Stoner et al.*, 2004, 2007]. Bioturbational effects are estimated to be minimal from the sharp and well-defined abundance peaks of tephra shards of the tephra markers Hekla 1104 and Hekla 3 [*Kristjánsdóttir*, 2005; *Kristjánsdóttir et al.*, 2007].

[12] The new Mg/Ca-temperature calibrations are applied to Mg/Ca measurements from the top 4000 cal yr B.P. (top 8 m) of core MD99-2269. Two cm thick sample slices were wet sieved at >63 μm, dry sieved at >106 μm and picked for foraminifera. Where available, all three Arctic benthic species were analyzed, but this was not possible for all downcore samples. As with the modern samples, great care was taken to select only pristine looking tests with no signs of dissolution, fragmentation, or dirty chambers. Before trace element analysis, each sample went through the same cleaning procedure as the calibration samples. However, due to smaller initial sample sizes, *C. neoteretis* and *I. norcrossi*/*helenae* samples were subjected to a gentler cleaning where sonication time and reagents were scaled down from normal procedure to maximize sample recovery. This procedure has been successfully used for very small or fragile samples in the UCSB laboratory (D. K. Pak, personal communication). The modified cleaning is as follows: (1) seven

Table 3. Modern Sample Data From the B997 Shelf Sites

	Site Specifics										
Number	Core Site[b]	Depth	BWS,[c] psu	BWT,[c] °C	ICT,[d] °C	Number Run[e]	Recovery, %	Mg/Ca, mmol/mol	$\delta^{18}O_c$, ‰	$\pm\delta^{18}O_c$, ‰	Number Run[f]
				Islandiella norcrossi/helenae							
1	B997-317	501	34.88	−0.07	0.49	44	36	1.019	4.36	0.03	25
2	B997-317	501	34.88	−0.07	0.49	44	57	1.095	4.36	0.03	25
3	B997-318	455	34.87	0.05	0.57	47	38	1.113	4.30	0.01	23
4	B997-319	426	34.87	0.21	0.85	40	39	1.071	4.24	0.03	29
5	B997-319	426	34.87	0.21	0.85	40	45	1.091	4.24	0.03	29
6	B997-320	389	34.95	4.66	1.25	43	34	1.159	4.10	0.02	22
7	B997-321	483	34.87	0.22	0.21	30	17	1.104	4.43	0.07	27
8	B997-321	483	34.87	0.22	0.21	30	19	1.088	4.43	0.07	27
9	B997-324	278	35.00	5.52	4.01	28	45	1.390	3.53	0.04	23
10	B997-324	278	35.00	5.52	4.01	28	50	1.347	3.53	0.04	23
11	B997-326	362	34.78	2.04	1.77	66	61	1.215	3.96	0.02	24
12	B997-327	360	34.78	1.58	5.25	44	46	1.402	3.10	0.01	24
13	B997-327	360	34.78	1.58	5.25	53	48	1.469	3.10	0.01	24
14	B997-327	360	34.78	1.58	5.25	44	51	1.426	3.10	0.01	24
15	B997-330	162	34.86	5.28	1.85	43	28	1.084	3.94	0.03	34
				Melonis barleeanus							
1	B997-314	245	35.05	6.03	6.51	10	33	1.637	2.33	0.01	15
2	B997-314	245	35.05	6.03	6.51	10	45	1.685	2.33	0.01	15
3	B997-314	245	35.05	6.03	6.51	10	58	2.070	2.33	0.01	15
4	B997-315	211	35.05	6.04	6.15	15	55	1.795	2.37	0.02	25
5	B997-315	211	35.05	6.04	6.15	15	75	1.788	2.37	0.02	25
6	B997-316	637	34.88	−0.24	0.19	80	38	0.772	3.78	0.02	20
7	B997-317	501	34.88	−0.07	0.35	67	17	0.669	3.82	0.02	30
8	B997-318	455	34.87	0.05	0.59	45	8	0.782	3.72	0.02	35
9	B997-319	426	34.87	0.21	0.51	52	22	0.702	3.75	0.03	40
10	B997-319	426	34.87	0.21	0.51	52	30	0.686	3.75	0.03	40
	B997-320[a]	*389*	*34.95*	*4.66*		*45*	*0*	*2.964*	*3.32*	*0.02*	*16*
11	B997-321	483	34.87	0.22	0.35	38	30	0.716	3.82	0.04	30
12	B997-321	483	34.87	0.22	0.35	38	32	0.785	3.82	0.04	30
13	B997-324	278	35.00	5.52	4.15	45	46	0.898	2.92	0.02	20
14	B997-324	278	35.00	5.52	4.15	45	63	0.899	2.92	0.02	20
15	B997-326	362	34.78	2.04	1.31	32	26	0.765	3.5	0.01	33
16	B997-326	362	34.78	2.04	1.31	32	61	0.772	3.5	0.01	33
	B997-330	*162*	*34.86*	*5.28*		*52*	*0*	*1.659*	*3.63*	*0.03*	*12*
17	B997-337	220	35.07	6.25	6.35	9	44	1.870	2.37	0.01	14
18	B997-337	220	35.07	6.25	6.35	9	70	2.035	2.37	0.01	14
19	B997-343	279	35.09	6.42	6.95	38	46	1.648	2.24	0.03	20
20	B997-343	279	35.09	6.42	6.95	38	48	1.695	2.24	0.03	20
21	B997-343, 106–150 μm	279	35.09	6.42	6.95	94	10	1.604	2.24	0.03	20
22	B997-343, 150–250 μm	279	35.09	6.42	6.95	42	43	1.642	2.24	0.03	20
23	B997-343, 150–250 μm	279	35.09	6.42	6.95	42	54	1.590	2.24	0.03	20
24	B997-343, >250 μm	279	35.09	6.42	6.95	17	41	1.593	2.24	0.03	20
25	B997-343, >250 μm	279	35.09	6.42	6.95	17	54	1.680	2.24	0.03	20
26	B997-345	319	35.11	7.12	6.95	13	43	1.616	2.23	0.01	20
27	B997-345	319	35.11	7.12	6.95	13	47	2.214	2.23	0.01	20
28	B997-345	319	35.11	7.12	6.95	35	65	1.753	2.23	0.01	20
29	B997-348	327	35.12	6.80	6.55	49	40	1.258	2.35	0.04	30
	B997-349	*265*	*35.13*	*6.95*		*22*	*39*	*4.382*	*2.21*	*0.03*	*30*
30	B997-349	265	35.13	6.95	6.99	22	42	1.260	2.21	0.03	30
31	BS11-91-K15	445	34.75	0.96	NA	62	17	0.644	3.02	0.06	7
				Cassidulina neoteretis							
1	B997-314	245	35.05	6.03	5.07	86	15	1.241	3.02	0.02	21
2	B997-315	211	35.05	6.04	5.07	91	43	1.377	2.97	0.02	20
	B997-319	*426*	*34.87*	*0.21*		*71*	*5*	*0.916*	*3.81*	*0.04*	*25*
	B997-320	*389*	*34.95*	*4.66*		*111*	*6*	*1.594*	*3.26*	*0.02*	*30*
3	B997-321	483	34.87	0.22	1.43	106	18	1.000	3.88	0.01	29

Table 3. (continued)

	Site Specifics										
Number	Core Site[b]	Depth	BWS,[c] psu	BWT,[c] °C	ICT,[d] °C	Number Run[e]	Recovery, %	Mg/Ca, mmol/mol	$\delta^{18}O_c$, ‰	$\pm\delta^{18}O_c$, ‰	Number Run[f]
4	B997-324	278	35.00	5.52	3.87	65	51	1.286	3.32	0.03	38
5	B997-326	362	34.78	2.04	2.07	50	31	0.987	3.64	0.04	25
6	B997-327	360	34.78	1.58	4.51	113	36	1.158	3.04	0.02	18
	B997-330	*162*	*34.86*	*5.28*		*143*	*5*	*0.988*	*3.34*	*0.01*	*27*
7	B997-337	220	35.07	6.25	5.47	64	30	1.355	2.92	0.02	24
8	B997-337	220	35.07	6.25	5.47	64	45	1.379	2.92	0.02	24
9	BS11-91-K15	445	34.75	0.96	NA	64	25	0.927	3.64	0.02	25
10	BS11-91-K15	445	34.75	0.96	NA	64	39	0.933	3.64	0.02	25

[a] Italic samples were not used for the Mg/Ca-temperature calibration.
[b] B997 Iceland shelf, BS11-91 Greenland shelf. See Table 2 for location.
[c] BWS, bottom water salinity, and BWT, bottom water temperature, from B997-CTD.
[d] ICT, isotopic calcification temperature, was calculated using *Shackleton* [1974] linear equation for low temperatures (see text).
[e] Number of foraminifera run for trace element analysis.
[f] Number of foraminifera run for isotopic analysis.

aggregate rinses with ultrasonication time of 15–25 sec, (2) 50 μl of hydrazine solution in a hot water bath for 30 min, without sonication, (3) 100 μl of buffered peroxide for 10 min without sonication, (4) 250 μl, 100 μl or no weak acid leach, depending on the size of the remaining sample. Cleaned samples were run on an ICP-MS at the University of California, Santa Barbara. Analytical error for Mg/Ca, Fe/Ca, Al/Ca, and Mn/Ca is the same as for the modern samples (see section 3.1). In addition, Sr, Na, Ba, La, Ce, Nd, and U were measured but are not reported here. Only Mg/Ca results with >10% recovery were used, because low recovery samples of *C. neoteretis* tended to be anomalously low in Mg/Ca (see later discussion). Here recovery is a percentage of the total weight of the sample prior to cleaning, and represents loss of sample due to the cleaning.

3.4. Benthic Species Picked

[13] We concentrate on three benthic species: *Islandiella norcrossi/helenae, Melonis barleeanus*, and *Cassidulina neoteretis* (Figure 4), which are all common on the Iceland shelf today [*Jennings et al.*, 2004]. *Islandiella norcrossi* and *Islandiella helenae* are very similar and are often combined in faunal assemblage analysis [*Rytter et al.*, 2002]; we combine the two species in order to maximize sample size. *I. norcrossi* is generally more common than *I. helenae* on the Iceland shelf [*Rytter et al.*, 2002]. Data from the Barents and Kara Seas suggest *I. norcrossi* is dependent upon seasonal blooms of organic productivity rather than temperature, salinity or substrate type [*Hald and Steinsund*, 1996]. However, it does prefer relatively low temperatures [*Hald and Steinsund*, 1996] and is generally assumed to have an infaunal microhabitat. *I. norcrossi*/*helenae* in the modern Iceland shelf samples has a very robust, hyaline test of translucent to slightly white color. Modern individuals on the Iceland shelf are usually >150 μm in size, with an average weight of 7 ± 1 μg.

[14] *Melonis barleeanus* has an intermediate to deep infaunal microhabitat [*Corliss*, 1985; *Corliss and Chen*, 1988; *McCorkle et al.*, 1990; *Wollenburg and Mackensen*, 1998; *Mackensen et al.*, 2000] and thrives on altered organic matter buried in the sediment [*Caralp*, 1989a, 1989b; *Wollenburg and Mackensen*, 1998]. Evidence from stable isotopes suggests it prefers a rather static position within the sediment [*Mackensen et al.*, 2000]. *M. barleeanus* is the most common and abundant species on the north Iceland shelf [*Rytter et al.*, 2002] and is especially dominant on the outer north Iceland shelf (Figure 4b), which has cool bottom waters of Upper Arctic Intermediate Water characteristics [*Jennings et al.*, 2004]. *M. barleeanus* in the modern Iceland shelf samples is generally of pinkish brown color, >150 μm, and has an average weight of 15 ± 8 μg.

[15] *Cassidulina neoteretis* [*Seidenkrantz*, 1995] is an indicator of chilled Atlantic Water (similar to what is carried in the NIIC) with normal salinity and low turbidity [*Jennings and Helgadóttir*, 1994; *Seidenkrantz*, 1995; *Hald and Steinsund*, 1996]. *C. neoteretis* is an infaunal species (generally assumed to be shallow infaunal) which responds to phytoplankton blooms [*Gooday and Lambshead*, 1989]. It is dominant on the inner north Iceland shelf where NIIC forms the bottom water mass as opposed to the dominance of

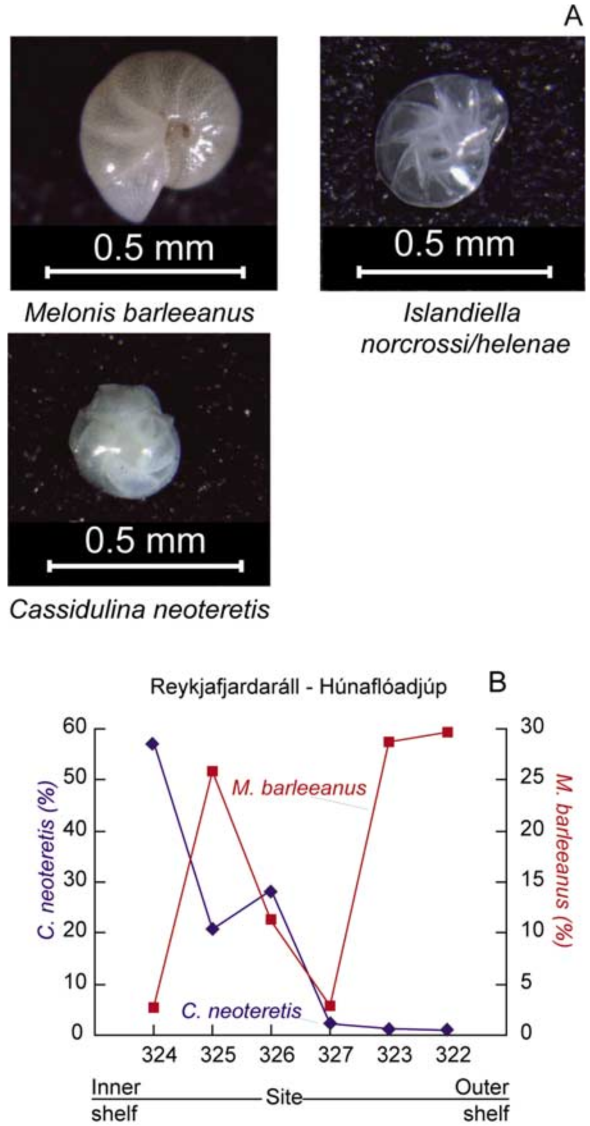

Figure 4. (a) Photographs of the three benthic species used in this study. *M. barleeanus* has a pinkish brown color, *I. norcrossi/helenae* has a clear/translucent color, and *C. neoteretis* has a translucent to milky white color. (b) Data from *Jennings et al.* [2004] showing the switch in dominance between *C. neoteretis* (blue diamonds) on the inner north Iceland shelf (site 324-326) to *M. barleeanus* (red squares) on the outer north Iceland shelf (site 327-322).

M. barleeanus on the outer north Iceland shelf (Figure 4b). *C. neoteretis* is often associated with fine-grained, organic rich, terrigenous mud [*Mackensen and Hald*, 1988]. The milky or semitranslucent tests of *C. neoteretis* specimens are small and thin-walled in the modern Iceland shelf samples (in contrast to the larger and more robust specimens found in the deglacial [*Jennings et al.*, 2006]). The modern *C. neoteretis* are usually <100–150 μm in size with an average weight of only 3 ± 1 μg per individual.

4. Calibration of Modern, Surface-Sediment Samples

4.1. Modern, Surface Sample Results

[16] The CTD temperature range captured by our calibration sites ranged from −0.2 to 7.1°C (Table 2). Measured δ^{18}O on bottom waters and benthic foraminifera yield an isotopic calcification temperature (see below) in the range of 0.2 to 7.0°C (Table 3). Mg/Ca in the modern samples varied from 0.64 to 2.21 mmol/mol (Table 3, Figure 5). A total of fifteen *I. norcrossi/helenae* samples from 9 Iceland shelf sites are included in the *I. norcrossi/helenae* calibration. All *I. norcrossi/helenae* samples had high recoveries after the cleaning because of their robust test structure. Thirty-one *M. barleeanus* samples from 15 sites are included in the *M. barleeanus* calibration. One site is located on the Greenland shelf. Two samples were omitted from the calibration due to low sample recovery after cleaning and one high outlier (4.38 mmol/mol, site 349) was also omitted. A total of ten samples, from eight sites, are included in the *C. neoteretis* calibration. One site is located on the Greenland shelf. Three samples were omitted due to low sample recoveries (Table 3). *C. neoteretis* is markedly smaller and lighter than the other two species so we had to run between 64–143 specimens for each sample compared to 28–66 for *I. norcrossi/helenae* and 9–80 for *M. barleeanus*.

[17] Of the three species, *M. barleeanus* spans the largest spatial range covering the region from the southwest to the north shelf (Jökuldjúp to Eyjafjardaráll). *C. neoteretis* is found on the north and northwest shelf (Eyjafjardaráll to Djúpáll), while *I. norcrossi/helenae* is only found on the north shelf (Reykjafjardaráll and Eyjafjardaráll) [*Jennings et al.*, 2004] (Figure 1). All three species have lower Mg/Ca for the colder north shelf sites than for the warmer southwest, west, and northwest sites in accordance with the postulated temperature control on Mg/Ca. There are also consistent spatial variations in the other elements but discussion of these variations in regards to a possible microhabitat effect (P. Martin, personal communication) is beyond the scope of this paper.

[18] Arctic foraminifera are in general smaller than their tropical counterparts. One advantage of the larger number of tests needed for each measure-

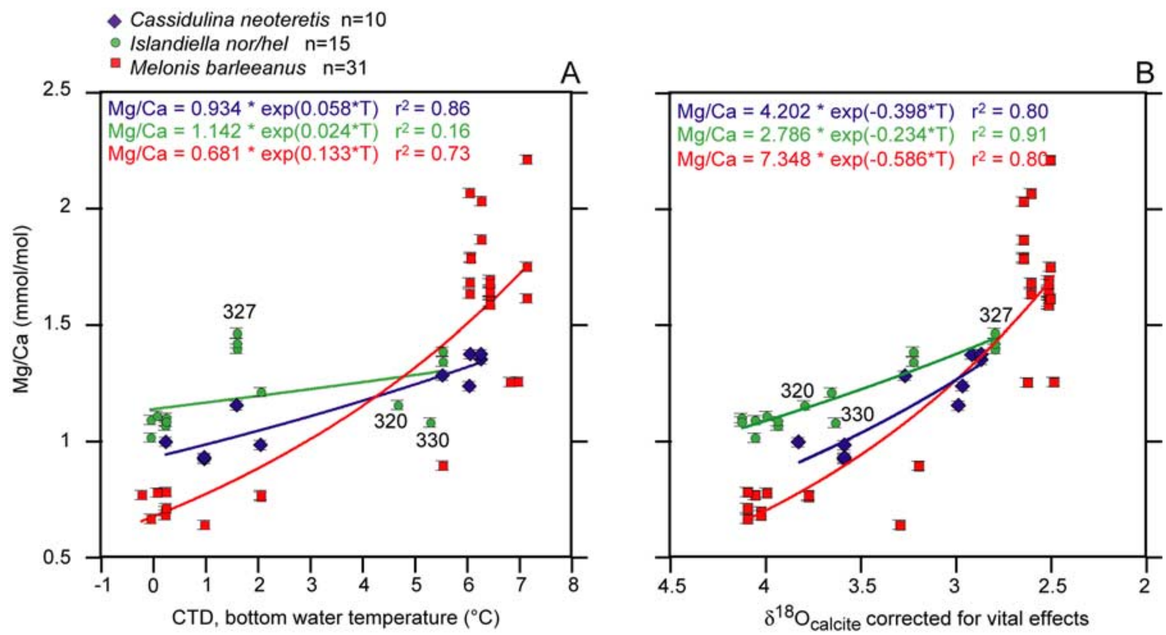

Figure 5. All modern Mg/Ca values plotted versus (a) bottom water temperature from the B997 CTD casts and (b) $\delta^{18}O_{calcite}$ corrected for vital effects (see text). Analytical error on the Mg/Ca measurements is 0.02 mmol/mol. *I. norcrossi*/*helenae* and *C. neoteretis* clearly have different Mg/Ca values than *M. barleeanus* supporting species-specific effects of Mg incorporation into foraminiferal calcite. Sites B997-320, −327, and −330 are offset from the general *I. norcrossi*/*helenae* trend when plotted versus CTD temperature (in contrast to their tighter distribution when plotted against isotopic calcification temperature in Figure 7).

ment (Tables 3 and 4) is that we obtain a more consistent value for Mg/Ca of the sample. A disadvantage is that it is difficult to obtain the required sample weight with the small tests and it is often impossible to stay within one narrow size fraction. However, the limited size fraction data available for benthic foraminifera do not show a consistent trend between size and Mg/Ca [*Raja et al.*, 2005; *Toyofuku and Kitazato*, 2005; *Rosenthal et al.*, 2006] (an exception is a culture study by *Hintz et al.* [2006a]). To test for possible size biases in the benthic foraminifera species of this study we used several samples from SW Iceland shelf site B997-343 (Figure 1b, Table 3) and core MD99-2269 (Table 4). We did not find a consistent trend between different sizes (size fractions defined by dry sieving) and Mg/Ca of *M. barleeanus* or *I. norcrossi*/*helenae* (Figure 6a). The >250 μm fraction has a greater spread of values than the smaller size fractions. The greater number of tests needed in the <250 μm yields a more consistent average value than the >250 μm size fraction. All size fractions (of a single sample) reconstructed the same temperature within calibration error of the species-specific temperature calibrations (Figure 6b).

4.2. Temperature Calibrations, CTD Temperature Versus Isotopic Calcification Temperature

[19] We initially calibrated Mg/Ca against July bottom water temperature obtained from the CTD casts taken during the B997 cruise (Figure 5a). Most samples showed increasing Mg/Ca with increasing temperature. Exceptions were samples from three northern shelf sites marked in Figure 5a (320, 327, and 330). However, if Mg/Ca is plotted against $\delta^{18}O_{calcite}$ the r^2 for the *I. norcrossi*/*helenae* trendline increases from 0.16 to 0.91 (Figure 5). It is clear from Figure 5b that higher Mg/Ca is associated with lower $\delta^{18}O_{calcite}$ (i.e., warmer temperatures) and thus we conclude that the measured foraminifera must not have been calcifying solely at the time the CTD temperature was measured (July 1997). The three sites under question are located where the two north Iceland shelf currents, NIIC and EIC, intersect – in an area of very high annual and seasonal hydrographic variability. Additionally sites 327 and 330 are known to produce anomalous results in benthic foraminiferal assemblages [*Jennings et al.*, 2004] as well as Mg/Ca and $\delta^{18}O_{calcite}$ [*Kristjánsdóttir*, 2005]. Modern hydrographic measurements show that seasonal and

Table 4. Downcore Data for the Last 4000 Cal Yr B.P. From Core MD99-2269[a]

Number	Interval, cm	Depth,[b] cm	Cal Yr B.P.	Number of Forams Run	Recovery, %	Mg/Ca, mmol/mol	Pyrite[c]	Size, μm
				Islandiella norcrossi/helenae				
1	65–67	66	404	22	47	1.079		
2	85–87	86	461	19	19	1.143		
3	95–97	96	490	54	47	1.165		
4	100–102	101	504	51	25	1.264		
5	102–104	103	510	46	48	1.322		
6	105–107	106	518	62	37	1.196		
7	115–117	116	547	38	53	1.155		
8	125–127	126	576	66	57	1.260		
9	135–137	136	605	50	50	1.158		
10	145–147	146	635	37	40	1.165		
11	155–157	156	664	29	43	1.257		
12	165–167	166	704	38	43	1.268		
13	175–177	176	754	36	58	1.240		
14	185–187	186	802	32	47	1.244	x	
15	205–207	206	899	28	28	1.177	x	
16	215–217	216	947	18	45	1.140	x	
17	265–266	266	1250	35	37	1.261	x	
18	275–277	276	1284	32	27	1.260	x	
19	285–287	286	1317	37	51	1.302	x	
20	295–397	296	1351	44	46	1.305	x	
21	305–307	306	1385	23	48	1.365	x	
22	315–317	316	1418	88	58	1.383	x	
23	325–327	326	1452	60	63	1.211		
24	335–337	336	1486	54	38	1.285	x	
25	345–347	346	1519	69	65	1.303	x	
26	355–357	356	1576	36	43	1.275	x	
27	365–367	366	1657	40	51	1.223	x	
28	375–377	376	1738	32	49	1.283		
29	385–387	386	1818	34	40	1.287	x	
30	395–397	396	1899	29	34	1.183	x	
31	405–407	406	1980	40	53	1.224	x	
32	415–417	416	2048	31	59	1.265	x	
33	425–427	426	2098	35	62	1.290	x	
34	435–437	436	2148	35	32	1.293	x	
35	445–447	446	2197	35	55	1.231	x	
36	455–457	456	2247	38	37	1.198	x	
37	465–467	466	2298	32	44	1.404	x	
38	475–477	476	2348	33	46	1.274	x	
39	485–487	486	2398	37	56	1.315	x	
40	495–497	496	2449	34	51	1.300	x	
41	505–507	506	2499	35	39	1.195	x	
42	515–517	516	2550	30	32	1.241	x	
43	525–527	526	2600	36	45	1.230	x	
44	535–537	536	2651	32	36	1.181	x	
45	545–547	546	2701	39	28	1.277	x	
46	565–567	566	2810	29	23	1.257	x	
47	575–577	576	2888	31	44	1.227	x	
48	585–587	586	2965	34	28	1.240	x	
49	595–597	596	3043	38	35	1.289	x	
50	615–617	616	3198	35	43	1.229	x	
51	625–627	626	3277	34	26	1.207	x	
52	635–637	636	3351	35	57	1.289	x	
53	645–647	646	3412	38	27	1.213	x	
	655–657[d]	*656*	*3474*	*40*	*14*	*2.214*	*x*	
54	665–667	666	3536	37	27	1.294	x	
55	675–677	676	3598	38	42	1.269	x	
56	685–687	686	3660	38	27	1.196	x	
57	695–697	696	3722	40	33	1.213	x	
58	705–707	706	3784	40	53	1.302	x	
59	715–717	716	3805	37	25	1.255	x	

Table 4. (continued)

Number	Interval, cm	Depth,[b] cm	Cal Yr B.P.	Number of Forams Run	Recovery, %	Mg/Ca, mmol/mol	Pyrite[c]	Size, μm
60	725–727	726	3818	39	24	1.267	x	
61	735–737	736	3832	38	19	1.277	x	
62	755–757	756	3859	31	30	1.318	x	
63	765–767	766	3873	32	11	1.183	x	
	775–777	*776*	*3886*	*36*	*3*	*1.174*	*x*	
64	785–787	786	3900	36	38	1.238	x	
65	795–797	796	3913	38	27	1.285	x	
66	945–947	937	4472	40	36	1.310	x	150–250
67	945–947	937	4472	32	35	1.341	x	180–212
68	1750–1752	1718	9251	53	38	1.374	x	150–180
69	1750–1752	1718	9251	40	37	1.403	x	150–250
70	1750–1752	1718	9251	12	28	1.381	x	250–300
71	2088–2090	2056	10302	46	37	1.354		150–180
72	2088–2090	2056	10302	36	49	1.378		150–250
73	2088–2090	2056	10302	14	65	1.361		250–300
				Melonis barleeanus				
1	5–7	6	13	22	11	0.796		
	15–17	*16*	*99*	*22*	*7*	*0.721*		
2	25–27	26	185	38	24	0.786		
3	35–37	36	270	14	13	0.745		
4	55–57	56	375	43	34	0.719		
5	65–67	66	404	29	11	0.811		
6	75–77	76	433	34	20	0.727		
7	102–104	103	510	25	15	1.116		
8	125–127	126	576	21	38	0.877		
9	135–137	136	605	52	46	0.797		
10	175–177	176	754	19	24	0.817		
11	215–217	216	947	49	33	1.049	x	
12	225–227	226	995	22	12	0.900		
13	235–237	236	1043	18	19	1.100	x	
	255–257	*256*	*1171*	*16*	*6*	*0.932*	*x*	
14	285–287	286	1317	47	44	0.996	x	
15	295–297	296	1351	43	29	1.010	x	
16	305–307	306	1385	41	40	1.188		
17	315–317	316	1418	22	21	0.828		
18	325–327	326	1452	38	36	0.906		
19	335–337	336	1486	54	42	1.032	x	
20	345–347	346	1519	48	39	0.904	x	
21	355–357	356	1576	47	24	0.967	x	
22	365–367	366	1657	42	22	0.862	x	
23	395–397	396	1899	44	56	1.024	x	
24	405–407	406	1980	49	31	1.018	x	
25	415–417	416	2048	48	44	1.035	x	
26	425–427	426	2098	32	17	0.982	x	
27	435–437	436	2148	25	12	0.856	x	
28	445–447	446	2197	37	36	1.083	x	
	465–467	*466*	*2298*	*40*	*8*	*0.967*	*x*	
	475–477	*476*	*2348*	*27*	*9*	*1.032*	*x*	
29	485–487	486	2398	38	24	0.890	x	
	505–507	*506*	*2499*	*26*	*8*	*0.741*	*x*	
30	515–517	516	2550	31	13	0.893	x	
31	525–527	526	2600	29	18	0.876	x	
32	545–547	546	2701	37	31	0.945	x	
33	565–567	566	2810	31	11	0.994	x	
34	575–577	576	2888	42	24	0.903	x	
35	585–587	586	2965	38	19	0.953	x	
	595–597	*596*	*3043*	*35*	*41*	*34.438*	*x*	
36	615–617	616	3198	33	11	0.883	x	
37	635–637	636	3351	33	16	0.820	x	
38	655–657	656	3474	30	19	0.972	x	

Table 4. (continued)

Number	Interval, cm	Depth,[b] cm	Cal Yr B.P.	Number of Forams Run	Recovery, %	Mg/Ca, mmol/mol	Pyrite[c]	Size, μm
39	665–667	666	3536	43	17	0.936	x	
40	685–687	686	3660	42	19	0.959	x	
41	705–707	706	3784	24	15	1.097	x	
	715–717	*716*	*3805*	*26*	*1*	*0.808*	*x*	
	755–757	*756*	*3859*	*33*	*8*	*1.009*	*x*	
42	775–777	776	3886	21	25	1.113	x	
43	1750–1752	1718	9251	32	52	1.122	x	180–250
44	1750–1752	1718	9251	15	61	1.113	x	250–300
45	2088–2090	2056	10302	34	29	0.875		150–250
46	2088–2090	2056	10302	13	42	0.958		250–300
				Cassidulina neoteretis				
	5–7	*6*	*13*	*102*	*7*	*0.934*		
	35–37	*36*	*270*	*72*	*1*	*0.976*		
	55–57	*56*	*375*	*69*	*1*	*0.813*		
	95–97	*96*	*490*	*61*	*10*	*0.882*		
1	100–102	101	504	113	30	1.151		
2	102–104	103	510	80	14	1.132		
3	105–107	106	518	120	12	1.044		
	125–127	*126*	*576*	*81*	*5*	*0.854*		
4	135–137	136	605	106	14	1.031		
5	145–147	146	635	122	13	0.977		
	155–157	*156*	*664*	*101*	*6*	*4.145*		
	165–167	*166*	*704*	*78*	*1*	*21.534*		
	175–177	*176*	*754*	*83*	*4*	*0.911*		
6	185–187	186	802	121	11	1.015		
	195–197	*196*	*850*	*113*	*4*	*1.111*		
	205–207	*206*	*899*	*90*	*1*	*0.953*		
7	215–217	216	947	132	11	1.047		
8	225–227	226	995	112	12	1.041		
9	235–237	236	1043	116	17	1.044		
	245–247	*246*	*1091*	*117*	*5*	*0.964*	*x*	
10	255–257	256	1171	119	11	1.043		
	265–266	*266*	*1250*	*156*	*5*	*1.204*	*x*	
11	277–275	276	1284	163	11	1.177	x	
	295–297	*296*	*1351*	*156*	*4*	*1.146*	*x*	
12	305–307	306	1385	189	24	1.187	x	
13	315–317	316	1418	145	23	1.275	x	
14	325–327	326	1452	129	18	1.150	x	
15	335–337	336	1486	143	10	1.236	x	
	345–347	*346*	*1519*	*133*	*10*	*1.141*	*x*	
	355–357	*356*	*1576*	*127*	*9*	*1.270*	*x*	
16	365–367	366	1657	168	12	1.150	x	
17	375–377	376	1738	131	12	1.149		
18	385–387	386	1818	137	10	1.276	x	
19	395–397	396	1899	130	12	1.331	x	
20	405–407	406	1980	100	16	1.360	x	
21	415–417	416	2048	128	21	1.426	x	
22	425–427	426	2098	90	30	1.303	x	
23	435–437	436	2148	90	37	1.262	x	
24	445–447	446	2197	91	32	1.136	x	
25	465–467	466	2298	86	32	1.321	x	
	475–477	*476*	*2348*	*101*	*7*	*1.087*	*x*	
26	485–487	486	2398	98	44	1.229	x	
27	505–507	506	2499	85	29	1.310	x	
28	515–517	516	2550	95	27	1.250	x	
29	525–527	526	2600	94	33	1.273	x	
30	545–547	546	2701	80	15	1.085	x	
31	565–567	566	2810	95	11	1.057	x	
	575–577	*576*	*2888*	*80*	*8*	*1.178*	*x*	
32	585–587	586	2965	84	20	1.277	x	

Table 4. (continued)

Number	Interval, cm	Depth,[b] cm	Cal Yr B.P.	Number of Forams Run	Recovery, %	Mg/Ca, mmol/mol	Pyrite[c]	Size, μm
	595–597	*596*	*3043*	*100*	*9*	*1.281*	*x*	
33	615–617	616	3198	87	41	1.208	x	
34	635–637	636	3351	88	21	1.121	x	
	655–657	*656*	*3474*	*80*	*6*	*1.038*	*x*	
35	665–667	666	3536	81	24	1.262	x	
36	685–687	686	3660	82	23	1.215	x	
37	705–707	706	3784	97	37	1.253	x	
38	715–717	716	3805	105	37	1.228	x	
39	755–757	756	3859	95	42	1.167	x	
40	775–777	776	3886	87	32	1.373	x	

[a] Additional samples for size fraction analysis are shown at the end of the list for each species (depths >800 cm).
[b] Gap corrected depth, −9 cm after 937 cm, −9–4 cm after 1204 cm, −9–4–20 cm after 1457 cm [*Kristjánsdóttir et al.*, 2007; *Stoner et al.*, 2007].
[c] Samples with microscopically detectable pyrite are marked with "x"; the pyrite was not quantified.
[d] Italic samples were not included in the MD99-2269 time series.

annual temperature fluctuations in this area can range from <0 to 5°C depending on which water mass dominates at the seafloor http://www.hafro.is/Sjora/). For example, two years prior to cruise B997, particularly cold conditions prevailed in this area [*Malmberg and Jónsson*, 1997] (Figure 3). According to the age model for core MD99-2269 (located close to site 327) 1 cm of sediment at the top of the core corresponds to approximately 8 years. Given the observed high annual variability, an 8 year window can encompass considerable variability in temperature and salinity (Figure 3). It is thus not surprising that the geochemistry of the sample (which contained unstained as well as stained foraminifera) or the faunal composition of these samples do not reflect the 1997 B997-CTD temperature.

[20] To circumvent this problem of high variability sites we have opted to calibrate Mg/Ca content against isotopic calcification temperature (ICT) (Figure 7) rather than the measured CTD temperature. We have to make certain assumptions when calculating the isotopic calcification temperature but given the good correlation between Mg/Ca and $\delta^{18}O_{calcite}$ we believe this is a better choice than to use a measured CTD temperature which we know (from the $\delta^{18}O_{calcite}$) does not represent the temperature at the time of calcification of the foraminifera. Isotopic calcification temperature is calculated from measured $\delta^{18}O_{seawater}$ (Table 2) and $\delta^{18}O_{calcite}$ (Table 3). The $\delta^{18}O_{seawater}$ was measured in bottom waters in July 1997. The $\delta^{18}O_{seawater}$ is converted from VSMOW to VPDB by subtracting 0.27 ‰ [*Hut*, 1987]. No bottom water $\delta^{18}O_{seawater}$ measurements are available for site K15 on the Greenland shelf so the calibrations include the CTD temperature for this one site (Table 3). We use the measured B997 $\delta^{18}O_{seawater}$ to derive an isotopic calcification temperature even though temporal variability in $\delta^{18}O_{seawater}$ might have occurred since the foraminifera calcified. The $\delta^{18}O_{seawater}$, at the high variability northern sites, can vary from 0.15 to 0.3 ‰ between the cold and warmer bottom waters respectively (Table 2); this translates to a 0.6 °C difference in temperature and is much less than the seasonal/annual variability in temperature at the site (<0 to 5°C). To calculate the isotopic calcification temperature we use the linear "paleotemperature"-equation (for data <16.9°C) of *Shackleton* [1974]: $T^* = 16.9 - 4.0^* (\delta^{18}O_{calcite\ corrected\ for\ vital\ effect} - \delta^{18}O_{seawater})$. T* is the calculated isotopic calcification temperature in °C. $\delta^{18}O_{seawater\ VSMOW}$ is measured in bottom water samples from cruise B997 (see above) and $\delta^{18}O_{calcite}$ is the measured $\delta^{18}O$ of foraminifera calcite $_{VPDB}$ collected in 1997 after correction for vital effect/disequilibrium as follows: *I. norcrossi/helenae* $\delta^{18}O_{calcite\ VPDB} - 0.298$ (n = 9), *M. barleeanus* $\delta^{18}O_{calcite\ VPDB} + 0.276$ (n = 18), and *C. neoteretis* $\delta^{18}O_{calcite\ VPDB} - 0.047$ (n = 18) [*Kristjánsdóttir*, 2005]. These vital effects/disequilibrium corrections are directly relevant both in time and space to our Mg/Ca measurements because they are based on measured $\delta^{18}O_{calcite}$ and $\delta^{18}O_{seawater}$ values from samples collected during the B997-cruise on the Iceland shelf [*Kristjánsdóttir*, 2005]. The vital effects/disequilibrium values were calculated using: $\delta^{18}O_{calcite}$ (vital effect/disequilibrium) = $\delta^{18}O_{calcite\ measured} - \delta^{18}O_{calcite\ equilibrium}$, where $\delta^{18}O_{calcite\ equilibrium}$ is calculated by substituting temperature and $\delta^{18}O_{seawater}$ (measured in July 1997 during the B997 cruise) into the "paleotemperature" equation. We assume the disequilibrium

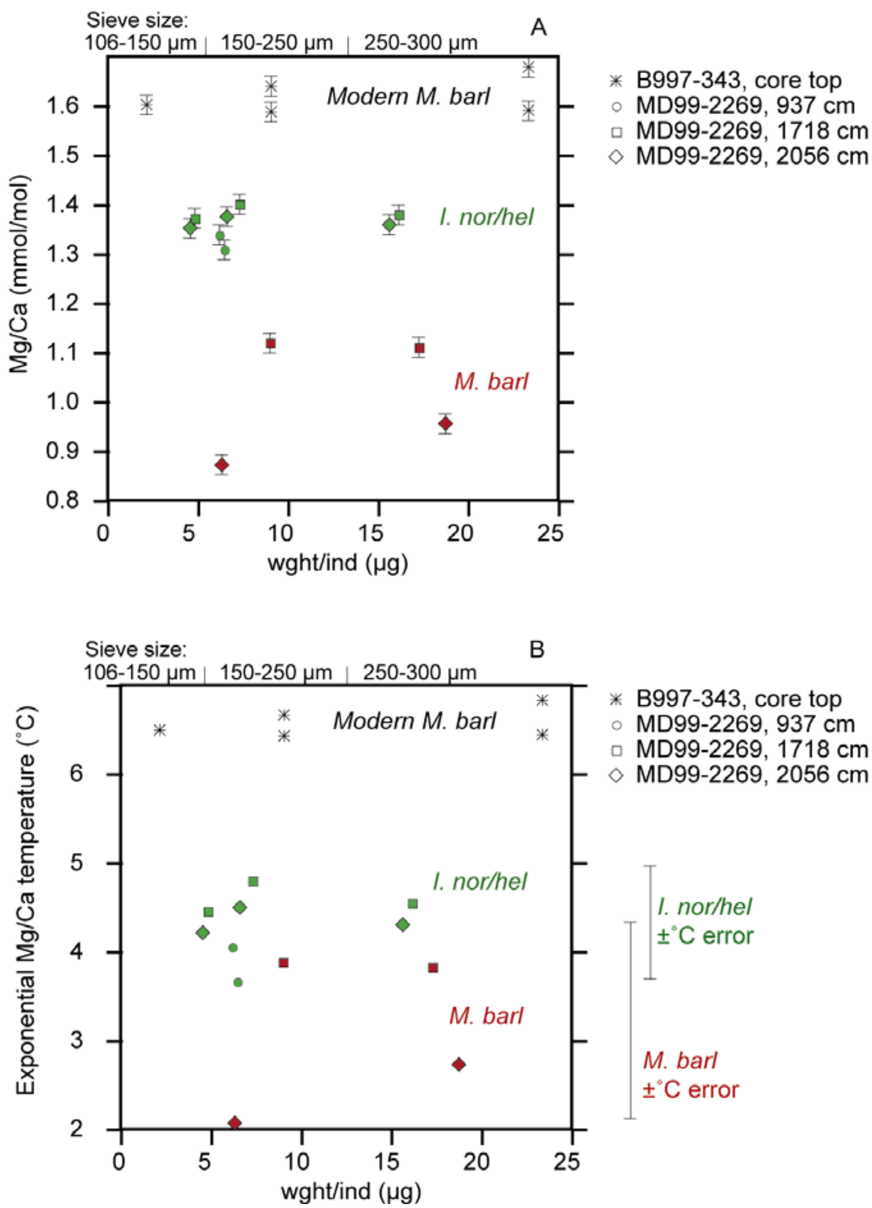

Figure 6. Shown are measurements of various size fractions of *M. barleeanus* and *I. norcrossi*/*helenae* from four different samples. Modern *M. barleeanus* are measured in samples from site B997-343, southwest Iceland shelf (black stars). Downcore *M. barleeanus* is measured in two samples, 1718 cm and 2056 cm, from core MD99-2269 (red symbols), and downcore *I. norcrossi*/*helenae* are measured in three samples, 937 cm, 1718 cm, and 2056 cm, from core MD99-2269 (green symbols). Top *x* axis shows the size of the sieve used for the dry sieving, whereas the bottom *x* axis shows the approximate weight of individual tests in μg (total weight of sample/number of foraminifera tests). (a) All but sample at 2056 cm overlap within Mg/Ca analytical error (0.02 mmol/mol). (b) All samples overlap within error when converted to temperature using the exponential species-specific equations (Table 1).

correction is constant because for the limited temperature range (<8°C) found on the Iceland shelf (1) all three species are linearly offset from calculated equilibrium values (using *Shackleton* [1974]: $T^* = 16.9 - 4.0 * (\delta^{18}O_{calcite\ corrected\ for\ vital\ effect} - \delta^{18}O_{seawater})$ and (2) the slopes of the relationships are not statistically different from the *Shackleton* [1974] equilibrium line [*Kristjánsdóttir*, 2005]. We believe the linear offset is justifiable for the small temperature range observed in this study. We can use other "paleotemperature" equations than *Shackleton* [1974] to calculate isotopic calcification temperature but this does not significantly alter the Mg/Ca-temperature calibration. As an example we

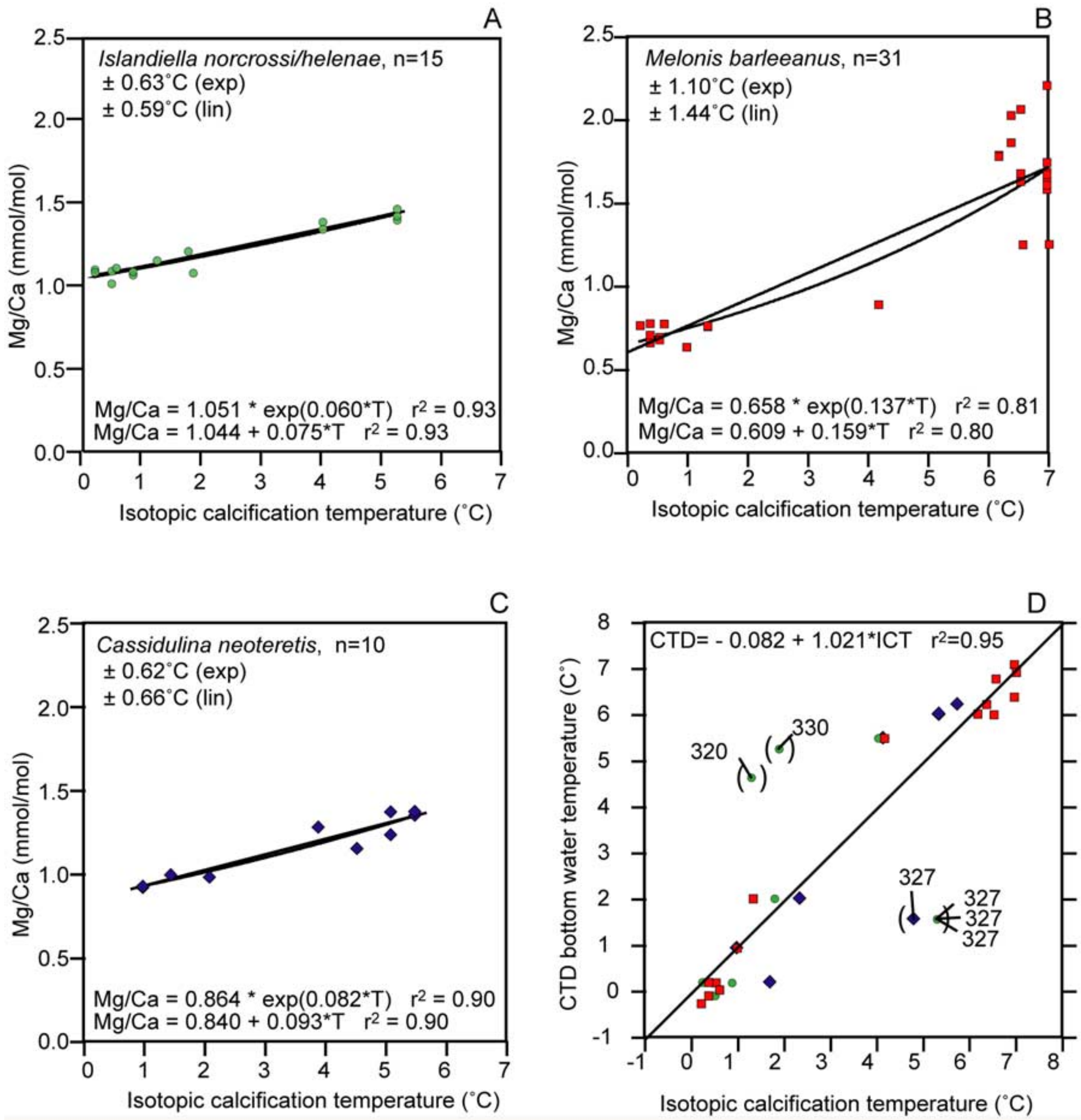

Figure 7. (a–c) Mg/Ca versus isotopic calcification temperature calibrations for the three benthic foraminifera species in this study. Both exponential and linear fits are shown. Standard error of the estimate is shown for both exponential and linear fits. Isotopic calcification temperature is calculated using T = 16.9 − 4.0 * ($\delta^{18}O_{calcite\ corrected\ for\ vital\ effect}$ − ($\delta^{18}O_{seawater}$) [*Shackleton*, 1974]. (d) Measured bottom water temperature (CTD) versus isotopic calcification temperature. If the sites (320, 327, and 330) with highest seasonal and annual temperature variability are excluded, then there is a very good correspondence between measured temperature (CTD) and calculated temperature (ICT).

show in Figure 8a the calibration based on ICT calculated using the *Shackleton* [1974] equation and the *Kim and O'Neil* [1997] calibration (*Kim and O'Neil* [1997]: T* = 16.10 − 4.64*($\delta^{18}O_{calcite\ corrected\ for\ vital\ effect}$ − $\delta^{18}O_{seawater}$) + 0.09 * ($\delta^{18}O_{calcite\ corrected\ for\ vital\ effect}$ − $\delta^{18}O_{seawater})^2$); vital effect/disequilibrium corrections are *I. norcrossi/helenae* $\delta^{18}O_{calcite\ VPDB}$ −0.769 (n = 9), *M. barleeanus* $\delta^{18}O_{calcite\ VPDB}$ −0.186 (n = 18), and *C. neoteretis* $\delta^{18}O_{calcite\ VPDB}$ − 0.504 (n = 18) [*Kristjánsdóttir*, 2005]. A regression between measured CTD temperature and isotopic calcification temperature for all three benthic species gives a relation close to 1:1 (CTD = − 0.082 + 1.021 * ICT, r^2 = 0.95) if we exclude the high variability sites of 320, 330 and 327 (Figure 7d).

[21] As a result of using calculated isotopic calcification temperature rather than measured bottom

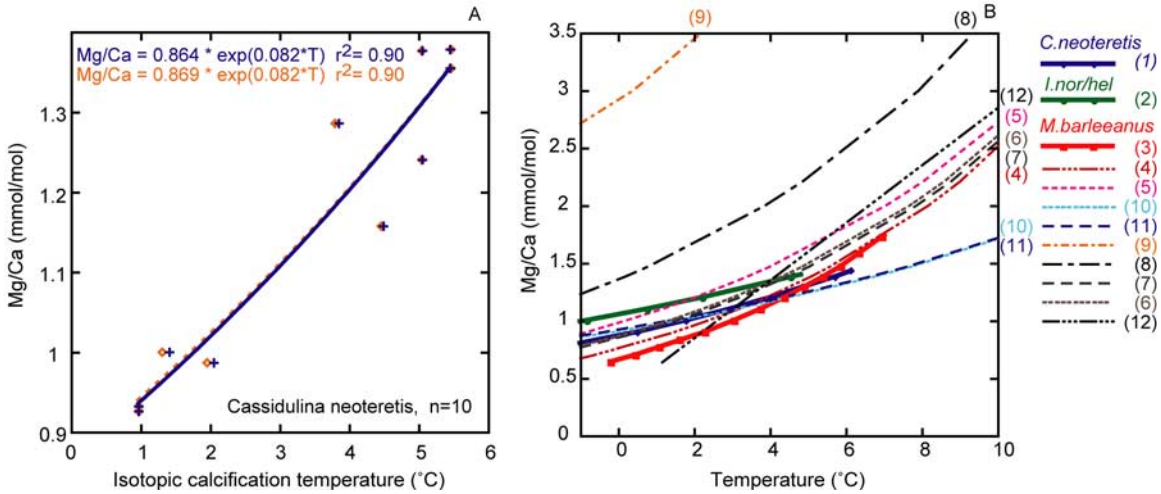

Figure 8. (a) *C. neoteretis* Mg/Ca versus isotopic calcification temperature calculated using two different paleotemperature equations (see text). T(°C) = 16.9 − 4($\delta^{18}O_{\text{calcite corrected for vital effect}} - \delta^{18}O_{\text{seawater}}$) [*Shackleton*, 1974] in blue and T(°C) = 16.1 − 4.64($\delta^{18}O_{\text{calcite corrected for vital effect}} - \delta^{18}O_{\text{seawater}}$) + 0.09($\delta^{18}O_{\text{calcite corrected for vital effect}} - \delta^{18}O_{\text{seawater}})^2$ [*Kim and O'Neil*, 1997] in orange. (b) The three benthic foraminifera calibrations from this study (1)–(3) compared to other benthic calibrations from the literature. For references and equations, see corresponding numbers in parentheses in Table 1.

water temperature from CTD, a better fit is obtained between the Mg/Ca ratios and temperature for *I. norcrossi*/*helenae* (compare Figure 5a and 7). Exponential fits and standard errors of estimate for our calibrations are shown in Table 1 and Figure 7. The exponential constant defines the temperature sensitivity of the calibration and thus the amplitude of the reconstructed temperature while the preexponential constant defines the absolute temperature values [*Lea*, 2003]. Exponential and preexponential error reported for this study is based on the 95% confidence interval. This study, as well as *Lear et al.* [2002], did not find any statistical evidence favoring linear fits rather than exponential fits for benthic calibrations. Therefore, by convention, we use the exponential calibrations, which conform to fundamental thermodynamic principles and have the advantage of parameterizing the Mg response as a percentage change (per 1°C), allowing direct comparison between different species [*Lea*, 2003]. All three benthic exponential fits are statistically different (using a t-test score) from each other, as are the linear fits. Both the linear and exponential fits have similar standard errors and would not give significantly different temperature changes if applied downcore.

4.3. Discussion of Modern, Surface Sample Results

[22] The three foraminifera species in this study have different microhabitat depths, but there does not seem to be any obvious relationship between microhabitat depths (infaunal versus epifaunal) and exponential or preexponential constants. The *I. norcrossi*/*helenae* (infaunal) and *C. neoteretis* (shallow infaunal) calibrations are similar to *Planulina ariminensis* (epifaunal) and *Uvigerina* spp. (infaunal) [*Lear et al.*, 2002] (Figure 8b), but different from the *Cibicidoides* spp. (epifaunal) [*Rosenthal et al.*, 1997; *Lear et al.*, 2002; *Martin et al.*, 2002] or *G. affinis* (deep infaunal) [*Skinner et al.*, 2003] fits (Table 1, Figure 8b). The *M. barleeanus* (deep infaunal) calibration has a relatively high exponential constant of 0.137 ± 0.020. This is higher than the 0.101 (no error estimate given) reported for *Melonis* spp. (n = 42) by *Lear et al.* [2002]. Despite this high exponential constant, our calibration reconstructs more realistic temperatures from our downcore record (see next section) than applying the *Lear et al.* [2002] multispecies calibration, which produces unrealistically cold (−3°C) temperatures. A monospecific *M. barleeanus* calibration using the 31 data points from this study (Table 3) along with 11 from the Bahamas, and 1 from the NE Atlantic (data from *Lear et al.* [2002]) results in a combination calibration for *M. barleeanus* of Mg/Ca = 0.757(±0.09) * exp(0.119 ± 0.014 * T), r^2 = 0.9, n = 43 (Table 1, (4) in Figure 8b) which overlaps within error with our *M. barleeanus* calibration. The exponential constant of the composite calibration (0.119 ± 0.014) (which covers a larger temperature range than our calibration) is lower and

more consistent with other benthic calibrations, but again is within error of the high exponential constant (0.137(±0.020)) of this study. Finally, we tried fitting the data with a fixed 0.1 exponential constant as demonstrated by *Anand et al.* [2003] but the fits significantly underperformed the prior calibrations. For this reason, we think that it is unlikely that one Mg/Ca-temperature relationship can describe all benthic foraminifera and that species-specific rather than genus-specific calibrations are needed. Standard errors of estimate for the new calibrations are from 0.63, 0.62, to 1.10°C for *I. norcrossi*/*helenae*, *C. neoteretis* and *M. barleeanus*, respectively. Potential sources of the calibration error include errors in estimating modern temperature, combining stained and unstained foraminifera, bioturbation, downslope transport, and varying growth rate between different environmental areas (kinetic effects). Our three calibrations cover an important temperature range for Mg/Ca calibrations, the <4°C, where previous work on deep sea depth-transects has suggested that carbonate saturation state may have a significant effect on Mg incorporation – possibly exceeding the temperature effect [*Martin et al.*, 2002; *Rosenthal et al.*, 2006; *Elderfield et al.*, 2006]. Our data do not show this steeper trend and we presume it is because the shallow sites are all supersaturated.

5. Applying the New Species-Specific Calibrations

5.1. Results From Core MD99-2269

[23] We measured Mg/Ca in samples from the top 4000 cal yr B.P. (top 8 m) in core MD99-2269 in order to compare the temperature reconstructions from the three different species. Sediment samples from every 10 cm were picked but it was not possible to find all three foraminifera species in sufficient quantities for geochemical analysis in every sample. The sample resolution thus varies between 6 and 232 years and is also variable between the different species, i.e., this is not a point-to-point comparison (Figure 9). The downcore *I. norcrossi*/*helanae* and *C. neoteretis* samples received a gentler cleaning than the modern samples whereas *M. barleeanus* received the full cleaning. The two cleaning methods produce very similar ranges of Mg/Ca ratios (Tables 3 and 4). We observe no change in recovery (as compared to the modern samples) of the robust *I. norcrossi*/*helanae* samples but do observe a decrease in recovery despite the modified cleaning for *C. neoteretis*. The lowest recovery *C. neoteretis* samples tend to be anomalously low in Mg/Ca (open symbols in Figure 9a), suggesting Mg-rich portions of the test may be lost due to over-cleaning. Because of this trend, any samples with recovery below 10% were excluded from this study (Table 4). All three benthic species have higher Mg/Ca values than planktonics in the same core (not shown), related to the generally higher preexponential constants that characterize benthic species [*Lea*, 2003]. As is observed with the modern samples, *I. norcrossi*/*helenae* has the highest Mg/Ca ratio, *C. neoteretis* has similar or somewhat lower ratio and *M. barleeanus* has the lowest values (Figure 9a). It should be noted that a slight trend is observed between Mg/Ca and Mn/Ca for *M. barleeanus* (Mg/Ca(mmol/mol) = 0.006(μmol/mol)Mn/Ca + 0.61, r^2 = 0.6) and *C. neoteretis* (Mg/Ca(mmol/mol) = 0.009(μmol/mol)Mn/Ca + 0.84, r^2 = 0.6) but no significant trend is noted for *I. norcrossi*/*helenae*. The samples at 664 cal yr B.P. (156 cm), 1350 cal yr B.P. (296 cm) (*I. norcrossi*/*helenae*), and 2810 cal yr B.P. (566 cm) (*M. barleeanus*) have anomalously high Fe/Ca values (>1000 μmol/mol) although their Mg/Ca values remain "normal." Pyrite was visually noted in many of the samples run for Mg/Ca, particularly in the older part of the interval studied (Table 4). Elemental results from these samples are not systematically different from the samples that did not contain any visible pyrite.

[24] Despite significantly different Mg/Ca ratios between the three benthic species (Figure 9a) the reconstructed temperature range is in good agreement with the seasonal and annual temperature ranges observed in the area today (Figures 2 and 9b). *I. norcrossi*/*helenae* and *M. barleeanus* reconstruct very similar temperature records throughout the last 4000 cal yr B.P. with temperature generally remaining below the NIIC Atlantic water threshold of 3.5°C (Figure 9b). All three species show similar temperatures and a cooling trend of approximately 0.1°C per century from circa 1500 - 0 cal yr B.P. (Figure 9) where *C. neoteretis* agrees well with the other two species (correlation coefficients > 0.30). However, from circa 1500 to 4000 cal yr B.P., *C. neoteretis* differs from the other two species averaging reconstructed temperature of 4.5°C (i.e., NIIC Atlantic water temperature) while *I. norcrossi*/*helenae* and *M. barleeanus* average 2.8 ± 0.8 and 2.5 ± 0.9°C respectively and correlation coefficients drop below 0.17. Periodically *C. neoteretis* reconstructs Arctic temperature more consistent with the other two species, for example at 2800 cal yr B.P. (2.5 ± 0.6°C).

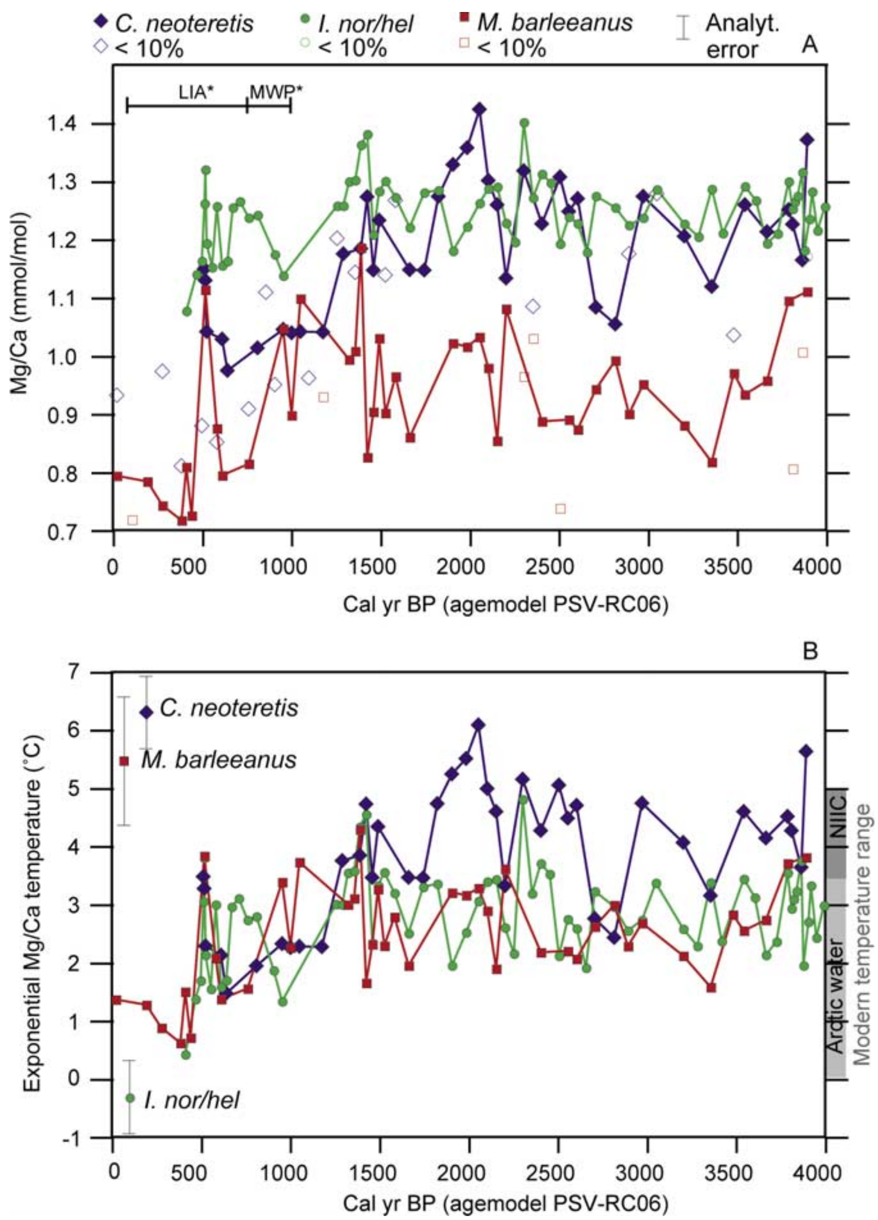

Figure 9. Time series from core MD99-2269 using age model PSV-RC06 [*Stoner et al.*, 2007]. *I. norcrossi*/*helenae*, green circles; *C. neoteretis*, blue diamonds; *M. barleeanus*, red squares. Two samples were eliminated from the *I. norcrossi*/*helenae* time series, one a high outlier, the other a low recovery sample (<10% recovery). Eight samples were eliminated from the *M. barleeanus* time series, one a high outlier and seven low recovery samples. The *C. neoteretis* time series suffered the greatest loss from low recovery samples; a total of 19 samples were eliminated (Table 4). Mg/Ca ratios in the remaining samples varied from 0.72 to 1.52 mmol/mol (Table 4). (a) Open symbols represent samples of less than 10% recovery. Mg/Ca analytical error 0.02 mmol/mol. Little Ice Age (LIA*) and Medieval Warm Period (MWP*) ages as designated by *Knudsen and Eiríksson* [2002]. (b) Temperature reconstructions (Mg/Ca > 10%) using the exponential species-specific Mg/Ca temperature calibrations (Table 1).

5.2. Discussion of Downcore Data

[25] The calibration and downcore trends for the three Arctic species reported here extend the observation that Mg incorporation into benthic foraminifera is species specific [*Lear et al.*, 2002; *Marchitto and deMenocal*, 2003; *Elderfield et al.*, 2006]. It is still unclear what controls this variability and whether it is only found in benthic foraminifera or also affects planktonic foraminifera. Due to the large diversity of benthic foraminifera [*Sen Gupta*, 1999] it is perhaps not surprising that differences exist in Mg incorporation. *Lear et al.*

[2002] state several possible causes for this observed difference, but they still remain speculative. Variable architecture of the tests of different foraminifera may influence the Mg incorporation. Co-precipitation experiments of inorganic calcite by *Paquette and Reeder* [1995] and *Reeder* [1996] have shown that trace element incorporation varies between crystallographic faces and even within some of the crystallographic faces, which can be affected by crystal size and shape. *Elderfield et al.* [1996] theorized that incorporation of trace elements into foraminiferal calcite is dependent upon different sizes of an internal calcification pool in foraminifera, differences in flushing time of that pool and differences in calcification rate. All these factors could differ between different benthic species.

[26] The large scale agreement of the three temperature reconstructions in the downcore record is encouraging. The decrease in bottom water temperatures after circa 1500 cal yr B.P. coincides nicely with an increase in abundance of Arctic benthic foraminifera species and increased occurrences of sea ice in the area (see next section). The observed divergence of *C. neoteretis* from the other two species circa 1500 to 4000 cal yr B.P. is intriguing and requires an explanation. We hypothesize here that temperature variations between the "growing" seasons of a single year (seasonal hydrographical variations) and/or between the same growing season of different years (multiannual hydrographical variations) may be responsible for the divergence of *C. neoteretis* from the other two species. On one hand *C. neoteretis* may be able to reproduce rapidly and under optimal conditions that differ from those of the other two species. If this were the case, its shell carbonate would record a different season or condition during the growing season. The preferred growing season of *C. neoteretis* on the Iceland shelf is unknown but we assume it reproduces in summer or fall when warmest temperature waters are observed. A dinocyst record from core B997-327PC (66°38′ N, 20°52′ W; water depth 373 m) [*Solignac et al.*, 2006] suggests a decrease in seasonality at circa 1500 cal yr when *C. neoteretis* converges again with the other two species. On the other hand, assuming that the three species have the same growing season, the divergence of *C. neoteretis* from the other two species may be related to the multiannual hydrographic variability of site MD99-2269 (Figure 3). A single sample from core MD99-2269 could be combining warm and cooler years into one sample, resulting in the observed divergence between the three benthic species. During times of less seasonal and/or multiannual variability, reconstructed temperature from *C. neoteretis* will be the same as that of *M. barleeanus* or *I. norcrossi*/*helenae*; for example at 2800 cal yr B.P. which also coincides with the first appearance, since its disappearance in early Holocene, of the Arctic foraminifera *Elphidium excavatum* (Figure 10b). Data on modern benthic foraminiferal fauna from the Iceland shelf indicate that *C. neoteretis* prevails in warmer inner shelf areas where the water column is dominated by NIIC Atlantic water, while *M. barleeanus* prevails in areas under the influence of colder Arctic intermediate water (Figure 4b) [*Jennings et al.*, 2004]. Present-day hydrography http://www.hafro.is/Sjora/) shows that variations of 2°C can occur between either the seasons of a single year (seasonal variations) and/or between the same seasons of different years (multiannual variations) making it difficult to distinguish seasonal variations from multiannual variations on the basis of temperature alone. Alternatively, poorly calibrated modern data or possible over-cleaning of the thin walled *C. neoteretis* could be responsible for the divergence rather than seasonal or annual hydrological changes.

5.3. Interpretation of Reconstructed Temperature Record

[27] The late Holocene on the north Iceland shelf is characterized by a general cooling trend toward the present, periodically interrupted by periods of warmer conditions [*Eiríksson et al.*, 2000; *Jiang et al.*, 2002; *Knudsen and Eiríksson*, 2002; *Castaneda et al.*, 2004; *Bendle and Rosell-Mele*, 2007]. This is also seen in our Mg/Ca-temperature reconstructions at site MD99-2269 (Figure 10) where all three benthic species show a cooling trend between circa 0–1500 cal yr B.P. with a decline in temperature by 0.1°C per century. We interpret this as evidence for decreased inflow of warm Atlantic water and increased inflow of colder Arctic water to the north Iceland shelf. This increase in Arctic water inflow is coincident with an increase in Arctic foraminiferal (*Giraudeau et al.* [2004] and A. E. Jennings (unpublished data)) and sea ice diatom assemblages [*Andersen et al.*, 2004; *Nowinski et al.*, 2004] as well as a rise in quartz, a proxy for sea ice in this area [*Moros et al.*, 2006] (Figure 10). However, two periods of Atlantic water interrupt the cooling at circa 500 cal yr B.P. (*M. barleeanus* 3.9 ± 1.1°C, *C. neoteretis* 3.3–3.5 ± 0.6°C, and *I. norcrossi*/*helenae* 3.1 ± 0.6°C) and 1400 cal yr B.P. (*M. barleeanus* 4.3 ± 1.1°C,

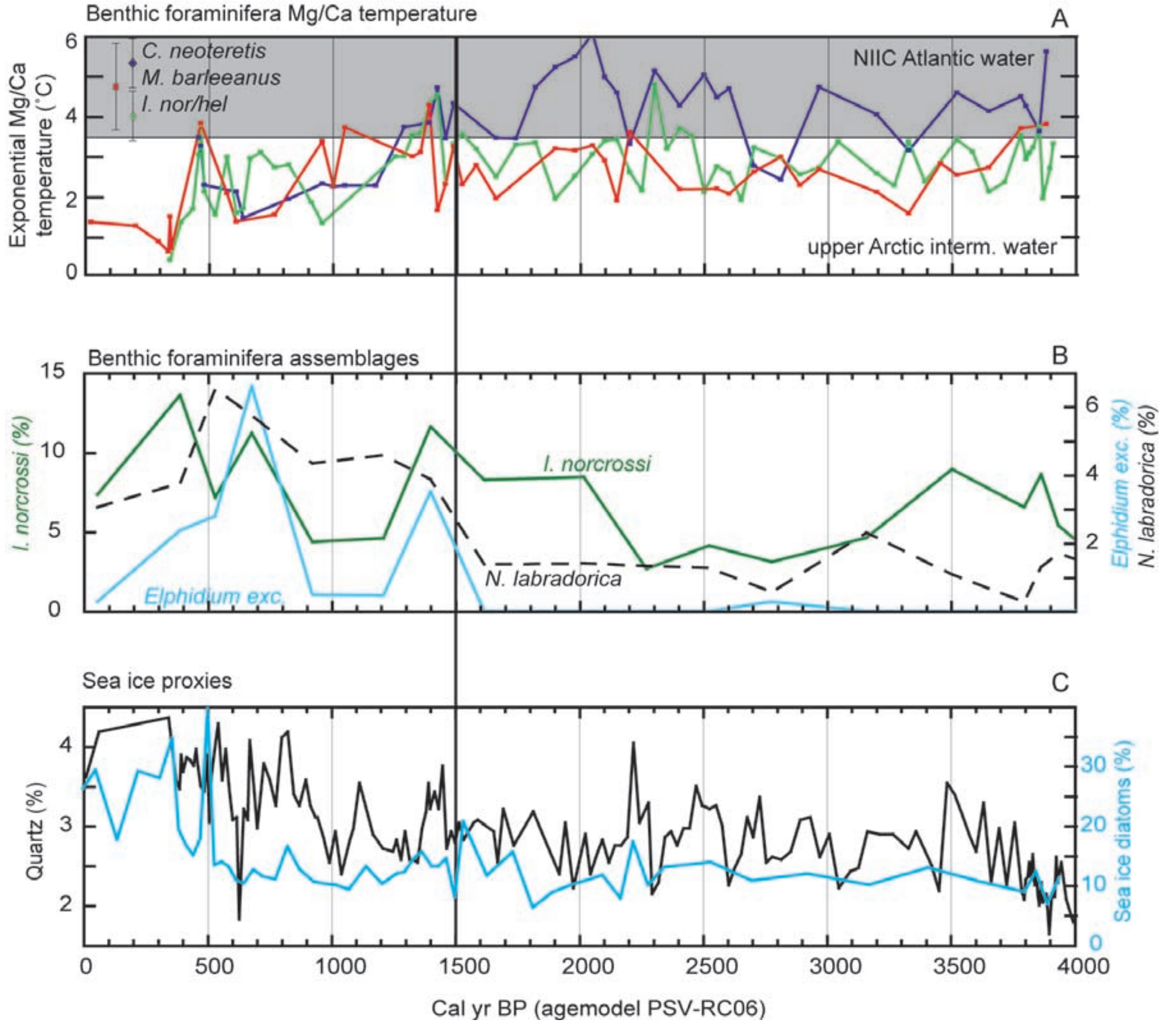

Figure 10. Various bottom and surface water proxies from core MD99-2269. (a) Bottom water temperature reconstruction from Mg/Ca ratios in benthic foraminifera (this study). Gray shading indicates Atlantic water of the NIIC. (b) Benthic foraminifera assemblage data for three Arctic foraminifera species [*Giraudeau et al.*, 2004; A. E. Jennings, unpublished data]. Notice the lower resolution (approximately every 250 years) of this data set. (c) Sea ice proxies from core MD99-2269. Quartz% from *Moros et al.* [2006] and diatom sea ice assemblage from *Andersen et al.* [2004] and *Nowinski et al.* [2004].

C. neoteretis 3.9–4.8 ± 0.6°C, and *I. norcrossi*/*helenae* 4.4–4.6 ± 0.6°C). No clear sign of warming during the Medieval Warm Period (circa 1000 cal yr B.P.) is recorded in the benthic record, this may be due to resolution problems. The lowest recorded reconstructed temperature, low abundances of foraminifera and generally small, light and fragile tests of benthic and planktonic foraminifera occur during the latter half of the Little Ice Age, as defined by *Knudsen and Eiríksson* [2002] (Figure 9a), whereas a short inflow event of Atlantic water is observed during the earlier part of the Little Ice Age (Figure 9b).

[28] Compared to the cooling trend observed in the record from 0–1500 cal yr B.P. a relatively stable, Arctic temperature regime is reconstructed from *M. barleeanus* and *I. norcrossi*/*helenae* between 1500 and 4000 cal yr B.P. The suggested presence of Arctic type bottom water (2–3°C) is similar to modern conditions (Figures 2a and 3). During this dominance of Arctic water, the reconstructed Mg/Ca-temperature of *M. barleeanus* and *I. norcrossi*/*helenae* indicates short periods of more Atlantic water influence (temperature >3.5°C) at circa 3850, 2400, and 2300 cal yr B.P. Additionally the divergence between *C. neoteretis* and the other two benthic foraminiferal species may suggest that

4000–1500 cal yr B.P. was a time of considerable seasonal and/or multiannual variability toward higher temperature on the north Iceland shelf (see previous section), which the *M. barleeanus* and *I. norcrossi*/*helenae* records are unable to capture on their own.

6. Conclusions

[29] Modern surface sediment samples from shallow sites (165 – 656 m) on the Iceland and Greenland shelves were used to create three new Mg/Ca-temperature calibrations for Arctic benthic foraminifera species. Mg/Ca was calibrated against isotopic calcification temperature rather than measured CTD temperature. All three species, *I. norcrossi/helenae, M. barleeanus*, and *C. neoteretis*, are infaunal shelf species. Mg incorporation is clearly species specific for these three species: *I. norcrossi*/*helenae* Mg/Ca = 1.051 ± 0.03 * exp(0.060 ± 0.011*T), r^2 = 0.93, SE = ±0.63°C; *M. barleeanus* Mg/Ca = 0.658 ± 0.07 * exp(0.137 ± 0.020 * T), r^2 = 0.81, SE = ±1.10°C; and *C. neoteretis* Mg/Ca = 0.864 ± 0.07 * exp(0.082 ± 0.020 * T), r^2 = 0.90, SE = ±0.62°C (Figure 7). *I. norcrossi*/*helanae* and *C. neoteretis* have fits that are similar to previously published fits of lower exponential constants for *P. ariminensis* and *Uvigerina* spp. [*Lear et al.*, 2002]. The *M. barleeanus* fit is different from *C. neoteretis* and *I. norcrossi*/*helenae* and more like published fits for *Cibicidoides* spp. [*Lear et al.*, 2002; *Martin et al.*, 2002] and *Melonis* spp. [*Lear et al.*, 2002]. These shallow water spatial calibrations do not show a steepening of the fit below 4°C as observed in some deep sea transects [*Martin et al.*, 2002; *Rosenthal et al.*, 2006; *Elderfield et al.*, 2006]. We presume this is because the shallow sites are situated in supersaturated waters. Preliminary tests on both modern and downcore samples indicate that size fractions within the range of Arctic samples, 106–300 μm, do not appear to significantly affect Mg/Ca incorporation. The three benthic calibrations were applied to Mg/Ca measurements of the three species in samples from core MD99-2269, located on the North Iceland shelf. The 4000 year long record from core MD99-2269 shows dominating Arctic water conditions from circa 4000–1500 cal yr B.P. The dominance of cooler bottom waters is periodically interrupted by influx of warmer (>3.5°C) Atlantic water of the North Iceland Irminger Current. Conditions cool further from circa 1500-0 cal yr B.P., culminating in the Little Ice Age. This cooling is supported by the coincident increase in Arctic foraminiferal fauna and increased evidence for sea ice occurrences in the same core [*Giraudeau et al.*, 2004; *Andersen et al.*, 2004; *Nowinski et al.*, 2004; *Moros et al.*, 2006]. An intriguing divergence of *C. neoteretis* from *M. barleeanus* or *I. norcrossi*/*helenae* is observed circa 1500 to 4000 cal yr B.P. where *C. neoteretis* reflects more Atlantic water conditions than do the other two species.

Acknowledgments

[30] We wish to thank the captain and crew of R/V *Marion Dufresne* on leg 3 of the IMAGES V cruise, John T. Andrews, David M. Anderson, Tom Marchitto, and Áslaug Geirsdóttir, for their contribution toward this project; A. Nowinski and N. Koc for supplying diatom data; Isla S. Castaneda for contributing photographs of the foraminifera; Árný E. Sveinbjörnsdóttir for running the $\delta^{18}O_{seawater}$ samples; Héðinn Valdimarsson for supplying Icelandic hydrographic data; Tara Chesley for assistance at the CU laboratory; and Georges Paradis for his guidance and hard work at the UCSB laboratory. The editors, David Hastings, Dan McCorkle, and an anonymous reviewer are thanked for their thoughtful and thorough review of this manuscript. Harry Elderfield is also thanked for giving up some of his time to discuss the implications of using ICT to construct Mg/Ca-temperature calibrations. This project was funded by two GSA Research Grants, 7186-02 and 7443-03, and NSF ESH grant ATM-0317832. University of Colorado Beverly Sears Graduate Student Grant also contributed toward this project. G. Paradis mass spectrometer operation at UCSB was supported in part by NSF grant OCE-0317611 (D.W.L.).

References

Aagaard, K., and L. K. Coachman (1968a), The East Greenland current north of the Denmark Strait: Part I, *Arctic*, *21*, 181–200.

Aagaard, K., and L. K. Coachman (1968b), The East Greenland current north of the Denmark Strait: Part II, *Arctic*, *21*, 267–290.

Anand, P., H. Elderfield, and M. H. Conte (2003), Calibration of Mg/Ca thermometry in planktonic foraminifera from a sediment trap time series, *Paleoceanography*, *18*(2), 1050, doi:10.1029/2002PA000846.

Andersen, C., N. Koç, A. Jennings, and J. T. Andrews (2004), Nonuniform response of the major surface currents in the Nordic Seas to insolation forcing: Implications for the Holocene climate variability, *Paleoceanography*, *19*, PA2003, doi:10.1029/2002PA000873.

Andrews, J. T., B. Larsen, K. Thors, G. Helgadóttir, J. Ólafsson, A. Wittmaack, E. Young, M. Daníelsson, D. Wilkens, and Z. Gosvig Larsen (1991), Cruise report - RS Bjarni Saemundsson BS1191, 1991 "Fjord-shelf-slope sediment continuum, East Greenland Margin," *Rep. Proj. A05/91 (NSF-DPP-9024100)*, 25 pp., Natl. Sci. Found., Arlington, Va.

Bendle, J. A. P., and A. Rosell-Mele (2007), High resolution alkenone sea surface temperature variability on the North Icelandic Shelf: implications for Nordic Seas paleoclimatic development during the Holocene, *Holocene*, *17*(1), 1–16.

Billups, K., and D. P. Schrag (2002), Paleotemperatures and ice volume of the past 27 Myr revisited with paired Mg/Ca and $^{18}O/^{16}O$ measurements on benthic foraminifera, *Paleoceanography*, *17*(1), 1003, doi:10.1029/2000PA000567.

Boyle, E., and L. D. Keigwin (1985/1986), Comparison of Atlantic and Pacific paleochemical records for the last 215,000 years: Changes in deep ocean circulation and chemical inventories, *Earth Planet. Sci. Lett.*, *76*, 135–150.

Boyle, E., and Y. Rosenthal (1996), Chemical hydrography of the South Atlantic during the last glacial maximum: Cd vs. $\delta^{13}C$, in *The South Atlantic: Present and Past Circulation*, edited by G. Wefer et al., pp. 423–443, Springer, New York.

Caralp, M. (1989a), Abundance of *Bulimina exilis* and *Melonis barleeanum*: Relationship to the quality of marine organic matter, *Geo Mar. Lett.*, *9*, 37–43.

Caralp, M. (1989b), Size and morphology of the benthic foraminifer *Melonis barleeanum*: Relationships with marine organic matter, *J. Foraminiferal Res.*, *19*, 235–245.

Castaneda, I. S., L. M. Smith, G. B. Kristjánsdóttir, and J. T. Andrews (2004), Temporal changes in Holocene $\delta^{18}O$ records from the northwest and central North Iceland shelf, *J. Quat. Sci.*, *19*, 321–334.

Corliss, B. H. (1985), Microhabitats of benthic foraminifera within deep-sea sediments, *Nature*, *314*, 435–438.

Corliss, B. H., and C. Chen (1988), Morphotype patterns of Norwegian Sea deep-sea benthic foraminifera and ecological implications, *Geology*, *16*, 716–719.

Eiríksson, J., K. L. Knudsen, H. Haflidason, and J. Heinemeier (2000), Chronology of late Holocene climatic events in the northern North Atlantic based on AMS ^{14}C dates and tephra markers from the volcano Hekla, Iceland, *J. Quat. Sci.*, *15*, 573–580.

Elderfield, H., C. J. Bertram, and J. Erez (1996), A biomineralization model for the incorporation of trace elements into foraminiferal calcium carbonate, *Earth Planet. Sci. Lett.*, *142*, 409–423.

Elderfield, H., J. Yu, P. Anand, T. Kiefer, and B. Nyland (2006), Calibrations for benthic foraminiferal Mg/Ca paleothermometry and the carbonate ion hypothesis, *Earth Planet. Sci. Lett.*, *250*, 633–649.

Epstein, S., and T. K. Mayeda (1953), Variations of the $^{18}O/^{16}O$ ratio in natural waters, *Geochim. Cosmochim. Acta*, *4*, 213–224.

Giraudeau, J., A. E. Jennings, and J. T. Andrews (2004), Timing and mechanisms of surface and intermediate water circulation changes in the Nordic Seas over the last 10000 years: A view from the North Iceland Shelf, *Quat. Sci. Rev.*, *23*, 2127–2139.

Gooday, A. J., and P. J. D. Lambshead (1989), Influence of seasonally deposited phytodetritus on benthic foraminiferal populations in the bathyal northeast Atlantic. The species response, *Mar. Ecol. Prog. Ser.*, *58*, 53–67.

Hald, M., and P. I. Steinsund (1996), Benthic foraminifera and carbonate dissolution in the surface sediments of the Barents and Kara Seas, in *Surface-Sediment Composition and Sedimentary Processes in the Central Arctic Ocean and Along the Eurasian Continental Margin*, *Ber. Polarforsch.*, vol. 212, edited by R. Stein et al., pp. 285–307, Alfred-Wegener-Inst. für Pol. und Meeresfordsch., Bremerhaven, Germany.

Helgadóttir, G. (1997), Paleoclimate (0 to > 14 ka) of W and NW Iceland: An Iceland/USA contribution to PALE, *Cruise Rep. B9-97 R/V Bjarni Sæmundsson RE30*, Rep. 62, Hafrannsóknastofnun (Mar. Res. Inst.), Reykjavik, 17–30 July.

Hintz, C. J., T. J. Shaw, J. M. Bernhard, G. T. Chandler, D. C. McCorkle, and J. K. Blanks (2006a), Trace/minor element:calcium ratios in cultured benthic foraminifera, Part II: Ontogenetic variation, *Geochim. Cosmochim. Acta*, *70*, 1964–1976.

Hintz, C. J., T. J. Shaw, G. T. Chandler, J. M. Bernhard, D. C. McCorkle, and J. K. Blanks (2006b), Trace/minor element:-calcium ratios in cultured benthic foraminifera. Part I: Interspecies and inter-individual variability, *Geochim. Cosmochim. Acta*, *70*, 1952–1963.

Hopkins, T. S. (1991), The GIN Sea—A synthesis of its physical oceanography and literature review 1972–1985, *Earth Sci. Rev.*, *30*, 175–318.

Hut, G. (1987), Consultants group meeting on stable isotope reference samples for geochemical and hydrological investigations, Int. At. Energy Agency, Vienna.

Izuka, S. T. (1988), Relationship of magnesium and other minor elements in tests of *Cassidulina subglobosa* and *C. oriangulata* to physical oceanic properties, *J. Foraminiferal Res.*, *18*, 151–157.

Jennings, A. E., and G. Helgadóttir (1994), Foraminiferal assemblages from the fjords and shelf of eastern Greenland, *J. Foraminiferal Res.*, *24*, 123–144.

Jennings, A. E., and N. J. Weiner (1996), Environmental change on eastern Greenland during the last 1300 years: Evidence from foraminifera and lithofacies in Nansen Fjord, 68°N, *Holocene*, *6*, 179–191.

Jennings, A. E., N. J. Weiner, G. Helgadóttir, and J. T. Andrews (2004), Modern foraminiferal faunas of the SW to N Iceland shelf: Oceanographic and environmental controls, *J. Foraminiferal Res.*, *34*, 180–207.

Jennings, A., M. Hald, M. Smith, and J. T. Andrews (2006), Freshwater forcing from the Greenland Ice Sheet during the Younger Dryas: Evidence from southeastern Greenland shelf cores, *Quat. Sci. Rev.*, *25*, 282–298.

Jiang, H., M.-S. Seidenkrantz, K. L. Knudsen, and J. Eiríksson (2002), Late-Holocene summer sea-surface temperatures based on a diatom record from the north Icelandic shelf, *Holocene*, *12*, 137–147.

Johannessen, O. M. (1986), Brief overview of the physical oceanography, in *The Nordic Seas*, edited by B. G. Hurdle, pp.103–127, Springer, New York.

Jónsson, S., and J. Briem (2003), Flow of Atlantic water west of Iceland and onto the north Iceland Shelf, *ICES Mar. Sci. Symp.*, *219*, 326–328.

Kim, S.-T., and J. R. O'Neil (1997), Equilibrium and nonequilibrium oxygen isotope effects in synthetic carbonates, *Geochim. Cosmochim. Acta*, *61*, 3461–3475.

Knudsen, K. L., and J. Eiríksson (2002), Application of tephrochronology to the timing and correlation of paleoceanographic events recorded in Holocene and Late Glacial shelf sediments off North Iceland, *Mar. Geol.*, *191*, 165–188.

Kristjánsdóttir, G. B. (2005), Holocene climatic and environmental changes on the Iceland shelf: $\delta^{18}O$, Mg/Ca, and tephrochronology of core MD99–2269, Ph.D. thesis, Univ. of Colo. at Boulder, Boulder.

Kristjánsdóttir, G. B., J. S. Stoner, A. Jennings, J. T. Andrews, and K. Grönvold (2007), Geochemistry of Holocene cryptotephras from the North Iceland Shelf (MD99–2269), Intercalibration with radiocarbon and paleomagnetic chronostratigraphies, *Holocene*, *17*(2), 155–157.

Labeyrie, L., E. Jansen, and E. Cortijo (2003), MD114/IMAGES V bord du Marion Dufresne, 1999, in *Rapports de Campagnes à la Mer*, edited by P.-E. Victor, *OCE/2003/02*, 850 pp., Inst. Pol. Fr. Paul-Émile Victor, Brest, France.

Lea, D. W. (2003), Elemental and isotopic proxies of past ocean temperatures, in *The Oceans and Marine Geochemistry*, edited by H. Elderfield, pp. 365–390, Elsevier, New York.

Lea, D. W., D. K. Pak, and G. Paradis (2005), Influence of volcanic shards on foraminiferal Mg/Ca in a core from the Galápagos region, *Geochem. Geophys. Geosyst.*, *6*, Q11P04, doi:10.1029/2005GC000970.

Lear, C. H., H. Elderfield, and P. A. Wilson (2000), Cenozoic deep-sea temperatures and global ice volumes from Mg/Ca in benthic foraminiferal calcite, *Science*, *287*(5451), 269–272.

Lear, C. H., Y. Rosenthal, and N. Slowey (2002), Benthic foraminiferal paleothermometry: A revised core-top calibration, *Geochim. Cosmochim. Acta*, *66*, 3375–3387.

Lear, C. H., Y. Rosenthal, and J. D. Wright (2003), The closing of a seaway: Ocean water masses and global climate change, *Earth Planet. Sci. Lett.*, *210*, 425–436.

Mackensen, A., and M. Hald (1988), *Cassidulina teretis* Tappan and *C. laevigata* D'Orbigny: Their modern and late Quaternary distribution in northern seas, *J. Foraminiferal Res.*, *18*, 16–24.

Mackensen, A., S. Schumacher, J. Radke, and D. N. Schmidt (2000), Microhabitat preferences and stable carbon isotopes of endobenthic foraminifera: Clue to quantitative reconstruction of oceanic new production?, *Mar. Micropaleontol.*, *40*, 233–258.

Malmberg, S.-A., and S. Jónsson (1997), Timing of deep convection in the Greenland and Iceland Seas, *ICES J. Mar. Sci.*, *54*, 300–309.

Malmberg, S.-A., and S. S. Kristmannsson (1992), Hydrographic conditions in Icelandic waters, 1980–1989, *ICES Mar. Sci. Symp.*, *195*, 76–92.

Marchitto, T. M., and P. B. deMenocal (2003), Late Holocene variability of upper North Atlantic Deep Water temperature and salinity, *Geochem. Geophys. Geosyst.*, *4*(12), 1100, doi:10.1029/2003GC000598.

Martin, P. A., and D. W. Lea (2002), A simple evaluation of cleaning procedures on fossil benthic foraminiferal Mg/Ca, *Geochem. Geophys. Geosyst.*, *3*(10), 8401, doi:10.1029/2001GC000280.

Martin, P. A., D. W. Lea, Y. Rosenthal, N. J. Shackleton, M. Sarnthein, and T. Papenfuss (2002), Quaternary deep sea temperature histories derived from benthic foraminiferal Mg/Ca, *Earth Planet. Sci. Lett.*, *198*, 193–209.

McCorkle, D. C., B. H. Corliss, and S. Emerson (1990), The influence of microhabitats on the carbon isotopic composition of deep-sea benthic foraminifera, *Paleoceanography*, *5*, 161–185.

Moros, M., J. T. Andrews, D. D. Eberl, and E. Jansen (2006), Holocene history of drift ice in the northern North Atlantic: Evidence for different spatial and temporal modes, *Paleoceanography*, *21*, PA2017, doi:10.1029/2005PA001214.

Nowinski, A., N. Koc, C. Andersen, A. Jennings, and J. S. Stoner (2004), Variability of the Irminger Current during the Holocene: Comparisons of the late and early Holocene periods, paper presented at 8th International Conference on Paleoceanography: An Ocean View of Global Change, Bordeaux I Univ., Biarritz, France.

Ólafsson, J. (1985), Recruitment of Icelandic haddock and cod in relation to variability in the physical environment, *ICES C. M. 1985/G:59*, Mar. Res. Inst., Reykjavik.

Ólafsson, J. (1999), Connections between oceanic conditions off N-Iceland, Lake Myvatn temperature, regional wind direction variability and the North Atlantic Oscillation, *Rit Fiskideildar*, *16*, 41–57.

Paquette, J., and R. J. Reeder (1995), Relationship between structure, growth mechanism, and trace element incorporation in calcite, *Geochim. Cosmochim. Acta*, *59*, 735–749.

Raja, R., P. K. Saraswati, K. Rogers, and K. Iwao (2005), Magnesium and strontium compositions of recent symbiont-bearing benthic foraminifera, *Mar. Micropaleontol.*, *58*, 31–44.

Rathburn, A. E., and P. De Deckker (1997), Magnesium and strontium composition of Recent benthic foraminifera from the Coral Sea, Australia and Prydz Bay, Antarctica, *Mar. Micropaleontol.*, *32*, 231–248.

Reeder, R. J. (1996), Interaction of divalent cobalt, zinc, cadmium, and barium with the calcite surface during layer growth, *Geochim. Cosmochim. Acta*, *60*, 1543–1552.

Rosenthal, Y., E. A. Boyle, and N. Slowey (1997), Temperature control on the incorporation of magnesium, strontium, fluorine, and cadmium into benthic foraminiferal shells from Little Bahama Bank: Prospects for thermocline paleoceanography, *Geochim. Cosmochim. Acta*, *61*, 3633–3643.

Rosenthal, Y., C. H. Lear, D. W. Oppo, and B. K. Linsley (2006), Temperature and carbonate ion effects on Mg/Ca and Sr/Ca ratios in benthic foraminifera: Aragonitic species *Hoeglundina elegans*, *Paleoceanography*, *21*, PA1007, doi:10.1029/2005PA001158.

Rytter, F., K.-L. Knudsen, M.-S. Seidenkrantz, and J. Eiríksson (2002), Modern distribution of benthic foraminifera on the North Icelandic shelf and slope, *J. Foraminiferal Res.*, *32*, 217–244.

Seidenkrantz, M.-S. (1995), *Cassidulina teretis* Tappan and *Cassidulina neoteretis* new species (foraminifera): Stratigraphic markers for deep sea and out shelf areas, *J. Micropaleontol.*, *14*, 145–157.

Sen Gupta, B. K. (1999), Introduction to modern foraminifera, in *Modern Foraminifera*, edited by B. K. Sen Gupta, pp. 3–6, Springer, New York.

Shackleton, N. J. (1974), Attainment of isotopic equilibrium between ocean water and the benthonic foraminifera genus Uvigerina: Isotopic changes in the ocean during the last glacial, *Cent. Natl. Rech. Sci. Collagues Int.*, *219*, 203–209.

Skinner, L. C., N. J. Shackleton, and H. Elderfield (2003), Millennial-scale variability of deep-water temperature and $\delta^{18}O_{dw}$ indicating deep-water source variations in the Northeast Atlantic, 0–34 cal. ka BP, *Geochem. Geophys. Geosyst.*, *4*(12), 1098, doi:10.1029/2003GC000585.

Solignac, S., J. Giraudeau, and A. de Vernal (2006), Holocene sea surface conditions in the western North Atlantic: Spatial and temporal heterogeneities, *Paleoceanography*, *21*, PA2004, doi:10.1029/2005PA001175.

Stoner, J. S., G. B. Kristjánsdóttir, A. Jennings, J. T. Andrews, J. Hardardóttir, and G. Dunhill (2004), Developing a Holocene chronostratgraphic template for the North Atlantic: Paleomagnetic, radiocarbon and tephra chronostratigraphies from Iceland (MD99–2269) and East Greenland (MD99–2322), *Eos Trans. AGU*, *85*(47), Fall Meet. Suppl., Abstract GP43B-0851.

Stoner, J. S., A. Jennings, G. B. Kristjánsdóttir, G. Dunhill, J. T. Andrews, and J. Hardardóttir (2007), A paleomagnetic approach toward refining Holocene radiocarbon-based chronologies: Paleoceanographic records from the north Iceland (MD99–2269) and east Greenland (MD99–2322) margins, *Paleoceanography*, *22*, PA1209, doi:10.1029/2006PA001285.

Swift, J. H., and K. Aagaard (1981), Seasonal transitions and watermass formation in the Iceland and Greenland seas, *Deep Sea Res., Part A*, *28*, 1107–1129.

Thordardóttir, T. (1977), Primary production in North Icelandic Waters in relation to Recent Climatic Change, paper presented at Polar Oceans, McGill Univ., Montreal, Canada, May 1974.

Toler, S. K., P. Hallock, and J. Schijf (2001), Mg/Ca ratios in stressed foraminifera, *Amphistegina gibbosa*, from the Florida Keys, *Mar. Micropaleontol.*, *43*, 199–206.

Toyofuku, T., and H. Kitazato (2005), Micromapping of Mg/Ca values in cultured specimens of the high-magnesium benthic foraminifera, *Geochem. Geophys. Geosyst.*, *6*, Q11P05, doi:10.1029/2005GC000961.

Toyofuku, T., H. Kitazato, H. Kawahata, M. Tsuchiya, and M. Nohara (2000), Evaluation of Mg/Ca thermometry in foraminifera: Comparison of experimental results and measurements in nature, *Paleoceanography*, *15*, 456–464.

Wollenburg, J., and A. Mackensen (1998), Living benthic foraminifers from the central Arctic Ocean: Faunal composition, standing stock and diversity, *Mar. Micropaleontol.*, *34*, 153–185.